# Visual Response Properties of Neurons in the LGN of Normally Reared and Visually Deprived Macaque Monkeys

JONATHAN B. LEVITT,[3] ROBERT A. SCHUMER,[3] S. MURRAY SHERMAN,[4] PETER D. SPEAR,[5] AND J. ANTHONY MOVSHON[1–3]

[1]*Howard Hughes Medical Institute,* [2]*Center for Neural Science, and* [3]*Department of Psychology, New York University, New York 10003;* [4]*Department of Neurobiology, State University of New York, Stony Brook, New York 11794-5230; and* [5]*Department of Psychology, University of Wisconsin, Madison, Wisconsin 53706*

Received 27 July 2000; accepted in final form 22 January 2001

**Levitt, Jonathan B., Robert A. Schumer, S. Murray Sherman, Peter D. Spear, and J. Anthony Movshon.** Visual response properties of neurons in the LGN of normally reared and visually deprived macaque monkeys. *J Neurophysiol* 85: 2111–2129, 2001. It is now well appreciated that parallel retino-geniculo-cortical pathways exist in the monkey as in the cat, the species in which parallel visual pathways were first and most thoroughly documented. What remains unclear is precisely how many separate pathways pass through the parvo- and magnocellular divisions of the macaque lateral geniculate nucleus (LGN), what relationships—homologous or otherwise—these pathways have to the cat's X, Y, and W pathways, and whether these are affected by visual deprivation. To address these issues of classification and *trans*-species comparison, we used achromatic stimuli to obtain an extensive set of quantitative measurements of receptive field properties in the parvo- and magnocellular laminae of the LGN of nine macaque monkeys: four normally reared and five monocularly deprived of vision by lid suture near the time of birth. In agreement with previous studies, we find that on average magnocellular neurons differ from parvocellular neurons by having shorter response latencies to optic chiasm stimulation, greater sensitivity to luminance contrast, and better temporal resolution. Magnocellular laminae are also distinguished by containing neurons that summate luminance over their receptive fields nonlinearly (Y cells) and whose temporal response phases decrease with increasing stimulus contrast (indicative of a contrast gain control mechanism). We found little evidence for major differences between magno- and parvocellular neurons on the basis of most spatial parameters except that at any eccentricity, the neurons with the smallest receptive field centers tended to be parvocellular. All parameters were distributed unimodally and continuously through the parvo- and magnocellular populations, giving no indications of subpopulations within each division. Monocular deprivation led to clear anatomical effects: cells in deprived-eye laminae were pale and shrunken compared with those in nondeprived eye laminae, and Cat-301 immunoreactivity in deprived laminae was essentially uniformly abolished. However, deprivation had only subtle effects on the response properties of LGN neurons. Neurons driven by the deprived eye in both magno- and parvocellular laminae had lower nonlinearity indices (i.e., summed signals across their receptive fields more linearly) and were somewhat less responsive. In magnocellular laminae driven by the deprived eye, neuronal response latencies to stimulation of the optic chiasm were slightly shorter than those in the nondeprived laminae, and receptive field surrounds were a bit stronger. No other response parameters were affected by deprivation, and there was no evidence for loss of a specific cell class as in the cat.

## INTRODUCTION

The visual pathways of mammals are organized into several parallel, largely independent neuronal streams from retina through the lateral geniculate nucleus (LGN) to visual cortex (Rodieck and Brening 1983; Sherman 1985; Stone 1983; Stone et al. 1979). These pathways differ in terms of their projection patterns, their neuronal morphology, and their cellular response properties. Presumably, each of these pathways is organized to perform somewhat different visual processing tasks for the animal (Lennie 1980; Shapley and Perry 1986; Sherman 1985; Stone 1983; Stone et al. 1979).

What remains uncertain is precisely how many of these separate pathways pass through the macaque's lateral geniculate nucleus and what relation these pathways have to the cat's W, X, and Y pathways. Initial analysis suggested that one pathway similar to the cat's X pathway passes through the parvocellular laminae and another similar to the cat's Y pathway passes through the magnocellular laminae (Dreher et al. 1976; Sherman et al. 1976). A putative third pathway, passing through the interlaminar zones of the primate LGN and encroaching somewhat into the parvo- and magnocellular laminae, remains incompletely characterized (Casagrande 1994; Fitzpatrick et al. 1983; Hendry and Yoshioka 1994). Kaplan and Shapley (1982) observed that the monkey's parvocellular laminae contain essentially only X cells of rather low visual sensitivity and that the magnocellular laminae contain a mixture of both X and Y cells of relatively high sensitivity. These authors concluded that the pathways passing through the monkey's magnocellular laminae are homologous to the X and Y pathways passing through the cat's A laminae. Shapley and Perry (1986) extended this *trans*-species comparison to suggest that the pathway involving the monkey's parvocellular geniculate laminae corresponds to the W pathway in the cat.

The resolution of this question would be facilitated by a more thorough classification of the neuron types found in these

Address for reprint requests: J. A. Movshon, Center for Neural Science, New York University, 4 Washington Place, Rm. 809, New York, NY 10003-6621 (E-mail: movshon@nyu.edu).

The costs of publication of this article were defrayed in part by the payment of page charges. The article must therefore be hereby marked "*advertisement*" in accordance with 18 U.S.C. Section 1734 solely to indicate this fact.

  

laminae. There is general agreement that cells in the parvocellular laminae are of a different class from those in the magnocellular laminae (Derrington and Lennie 1984; Dreher et al. 1976; Kaplan and Shapley 1982; Sherman et al. 1976; Spear et al. 1994). Kaplan and Shapley (1982) claim that the magnocellular laminae contain two cell classes, X and Y, which can be distinguished by several correlated parameters: the Y cells, which display nonlinear summation, have poorer spatial resolution and are innervated by faster conducting retinal axons than the X cells, which display linear summation. Derrington and Lennie (1984) found no evidence for two cell types among the neurons in their sample from the monkey's magnocellular laminae; a quantitative measure of the extent of nonlinear summation, the "nonlinearity index" of Hochstein and Shapley (1976), was unimodally distributed among these neurons, and no correlation was seen between the extent of nonlinear summation and spatial resolution. However, Derrington and Lennie (1984) emphasize that the sample size in both their study and that of Kaplan and Shapley (1982) precludes an unambiguous resolution of this matter of classification. More recently, Spear et al. (1994) described the response properties of a much larger sample of neurons in both the magno- and parvocellular laminae of macaque LGN. All response measures appeared continuously distributed; however, they did not determine the extent of nonlinear summation, which might have revealed subpopulations.

To address these issues, we used achromatic stimuli to measure a range of response properties from neurons in the parvo- and magnocellular laminae of the LGN of nine macaque monkeys: four raised normally and five monocularly deprived of vision by lid suture for at least five years starting near the time of birth. In cats, monocular deprivation produces a selective loss of Y cells and a reduction in spatial resolution among X cells in LGN laminae driven by the deprived eye (Lehmkuhle et al. 1980; Sherman and Spear 1982; Sherman et al. 1972). Studying the monocularly deprived monkey LGN might similarly indicate whether a particular cell type within the magno- or parvocellular laminae was affected or lost. A previous study (Blakemore and Vital-Durand 1986b) reported little difference between cells in layers driven by the two eyes in monocularly deprived old-world monkeys. However, they studied only one animal deprived for more than 70 days and made too few quantitative measurements on each cell to establish effects of deprivation specific to particular physiologically defined cell types. Our results show that parvo- and magnocellular neurons form two distinct and separate functional cell classes; we find no evidence using achromatic stimuli that these classes can usefully be subdivided. Monocular deprivation had only very subtle effects on the visual response properties of geniculate neurons and did not seem to have specific effects on any particular cell group.

We have briefly described some of these results in abstract form (Levitt et al. 1989; Sherman et al. 1984).

## METHODS

### *Surgical preparation and maintenance*

We performed these experiments on four normal young adult cynomolgus monkeys (*Macaca fascicularis*) and on five rhesus monkeys (*M. mulatta*) reared from birth to the age of 5–6 yr with the right eyelid sutured shut. All experimental procedures conformed to National Institutes of Health guidelines. Animals were initially premedicated with atropine (0.25 mg), and acepromazine maleate (0.05 mg/kg), or valium (Diazepam: 0.5 mg/kg). After induction of anesthesia with intramuscular injections of ketamine (Vetalar: 10–30 mg/kg), cannulae were inserted in the saphenous veins and surgery was continued under intravenous barbiturate anesthesia (sodium thiopental, Pentothal: 1–2 mg/kg boluses as needed). After cannulation of the trachea, the animal's head was fixed in a stereotaxic frame. A small craniotomy was made, and after making a small slit in the dura, a tungsten-in-glass microelectrode (Merrill and Ainsworth 1972) was positioned at stereotaxic coordinates A7 L11; the hole was then covered with warm agar. Bipolar stimulating electrodes (Rhodes Medical) were also implanted into the optic chiasm; the appropriate position was determined by recording evoked visual activity through the electrodes. Once correctly positioned, they were fixed to the skull with dental cement. On completion of surgery, animals were paralyzed to minimize eye movements. Paralysis was maintained with an infusion of pancuronium bromide (Pavulon: 0.1 mg $\cdot$ kg$^{-1}$ $\cdot$ h$^{-1}$) or vecuronium bromide (Norcuron: 0.1 mg $\cdot$ kg$^{-1}$ $\cdot$ h$^{-1}$) in lactated Ringer solution with dextrose (5.4 ml/h). Animals were artificially ventilated with room air or a 49:49:2 mixture of $N_2O$:$O_2$:$CO_2$. Peak expired $CO_2$ was maintained at 4.0% by adjusting the respirator stroke volume or the $CO_2$ content in the gas mixture. Rectal temperature was kept near 37°C with a thermostatically controlled heating pad. Anesthesia was maintained by continuous infusion of sodium pentobarbital (Nembutal: 1–2 mg $\cdot$ kg$^{-1}$ $\cdot$ h$^{-1}$). The electrocardiograph (EKG), electroencephalograph (EEG), and rectal temperature were monitored continuously to ensure the adequacy of anesthesia and the soundness of the animal's physiological condition. Animals also received daily injections of a broad-spectrum antibiotic (Bicillin: 300,000 U).

The pupils were dilated and accommodation paralyzed with topical atropine, and the corneas were protected with zero power contact lenses; supplementary lenses were chosen that permitted the best spatial resolution of recorded units. We opened the eyelids of the monocularly deprived animals on the day of the experiment and noted that while the deprived eye tended to be rather myopic relative to the nondeprived eye [in agreement with Wiesel and Raviola (1977), interocular differences ranging from 5 to 11.5 diopters], the quality of the deprived eye's optics was in every case excellent. Contact lenses were removed periodically for cleaning, and the eyes were rinsed with saline. The lenses were also removed for several hours each day, the eyes given a few drops of ophthalmic antibiotic solution (Gentamicin), and the lids closed. At the beginning of the experiment, and before beginning each day's recording, the foveas were located and plotted using a reversible ophthalmoscope.

### *Characterization of receptive fields*

Receptive fields were initially mapped by hand on a tangent screen using black-and-white or colored geometric targets. When a single neuron's activity was isolated, we established the eye through which it was driven and occluded the other for quantitative experiments. We classified each cell by the criteria of Wiesel and Hubel (1966) according to its receptive field organization and sensitivity to color, using four broadband gelatin (Wratten) filters (red, green, blue, and yellow). We also measured the cell's response latency to electrical stimulation of the optic chiasm, receptive field eccentricity, and whether it was on- or off-center. Following this initial characterization, we positioned the receptive field on the face of a display CRT, and quantitative experiments using sinusoidal grating stimuli proceeded under computer control. Achromatic stimuli (vertically oriented sinusoidal gratings) were presented within a circular region on the face of a Hewlett-Packard 1332A display oscilloscope with a P31 phosphor and a mean luminance of 40 cd/m$^2$; display contrast was linearly related to input voltage up to the maximum contrasts used. At the viewing distance of 57 cm, the screen subtended 9.5° at the monkey's eye. Stimulus presentation was controlled by a PDP11 computer, which also accu-

mulated, stored, and analyzed neuronal response data. Action potentials were conventionally amplified and displayed; standard pulses triggered by each impulse were stored by the computer and were also fed to an audiomonitor. A standard experimental procedure was followed for all cells encountered. Each experiment consisted of several (generally 4–10) blocks of trials. Within each block, all stimuli were presented for the same amount of time (generally 5–10 s); grating stimuli were either drifted or counterphase flickered with a sinusoidal time course. In each experiment, we measured responses by averaging several repeats of a randomly interleaved set of stimuli, and we always included a uniform field stimulus of the same duration and mean luminance as our grating stimuli to obtain an estimate of spontaneous activity. We Fourier-analyzed responses to determine the mean (F0), first harmonic (F1), and second harmonic (F2) components of the response as well as the temporal phase of each response component; except as specifically noted in the following text, we always measured response with the F1 component, that is, the amplitude of the response component that modulated in synchrony with the temporal modulation of the stimulus.

### *Neuroanatomical methods*

During recording, small electrolytic lesions were produced at locations of interest along the electrode track by passing DC current through the electrode tip (1–2 $\mu$A for 2–5 s, tip negative). At the end of the experiment, the animals were killed with an overdose of Nembutal and perfused transcardially with buffered formalin or 4% paraformaldehyde. Blocks containing the region of interest were sunk in the cold in a postfix solution containing 30% sucrose, after which 50-$\mu$m-thick coronal sections were cut on a freezing microtome. Sections were stained for Nissl substance with cresyl violet. Cells' laminar locations were determined by the stereotypical shift in eye preference as the electrode passed through each of the LGN laminae; recording sites were subsequently verified histologically. Selected tissue sections of interest were reacted to reveal Cat-301 immunoreactivity (Hendry et al. 1984, 1988; Hockfield et al. 1983). Briefly, tissue sections were incubated overnight in monoclonal antibody Cat-301 (full-strength supernatant) and then for 2–4 h in an appropriate dilution (1:50 or 1:100) of secondary antibody [affinity-purified rabbit anti-mouse conjugated with horseradish perioxide (HRP): Cappell]. HRP label was visualized with diaminobenzidine as the chromogen, then tissue sections were mounted on gelatin-coated slides, defatted, cleared, and coverslipped.

## RESULTS

Our sample consists of 468 geniculate neurons: 214 studied in the four normal animals and 254 neurons from the five monocularly deprived animals. We studied certain response parameters of these cells qualitatively, and we describe these before considering the more quantitative receptive field data. We will describe the results from normal and deprived animals together to demonstrate more clearly any possible subpopulations within the magnocellular or parvocellular laminae and to address the effects of deprivation. While we may have encountered a few koniocellular neurons, it is unlikely we recorded from many since they are so small and are restricted to the interlaminar zones. Values reported for each parameter are means ± SD, and we used Mann-Whitney *U* tests for all statistical comparisons between groups.

### *Neuroanatomical observations*

Figure 1 shows photomicrographs of coronal sections through the right hemisphere (ipsilateral to the sutured eye) of one of the deprived animals. Figure 1*A* is a Nissl-stained section. Cells in laminae innervated by the deprived eye (2, 3, and 5) were clearly pale and shrunken when compared with cells in nondeprived laminae as previously noted by many others (e.g., Headon and Powell 1973; Sherman and Spear 1982; Tigges et al. 1984; Vital-Durand et al. 1978; von Noorden and Crawford 1978). We also examined the pattern of Cat-301 immunoreactivity in the deprived animals' LGN since it preferentially labels magnocellular laminae in the monkey and Y cells in the cat LGN (Hendry et al. 1984, 1988; Hockfield and Sur 1990; Hockfield et al. 1983), and expression of this antigen in the cat is dependent on visual experience (Guimaraes et al. 1990; Sur et al. 1988). We therefore thought examining reactivity patterns in the deprived monkey LGN would confirm the efficacy of our deprivation regimen and suggest parallels with the functional organization of the cat LGN. Figure 1*B* shows Cat-301 immunoreactivity in a nearby section. Immunoreactivity is most intense in lamina 1, the nondeprived magnocellular lamina, though fainter reactivity can also be observed in the nondeprived parvocellular laminae 4 and 6 as well. Immunoreactivity is essentially eliminated in the deprived magnocellular lamina 2 as well as in the deprived parvocellular laminae 3 and 5.

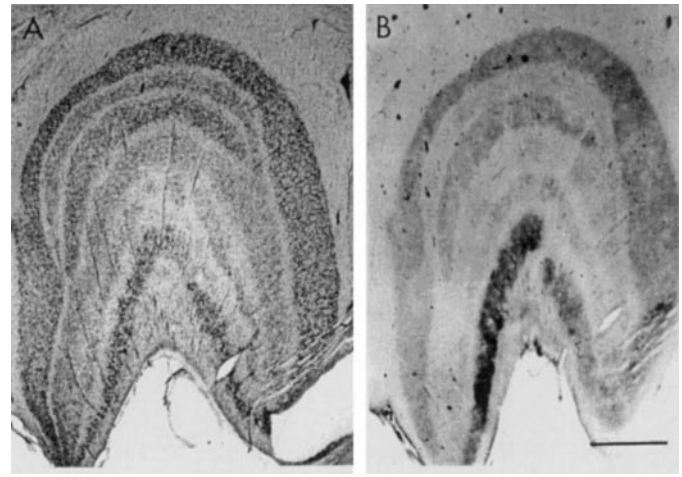


FIG. 1. Photomicrographs of Nissl (*A*)- and nearby Cat-301 (*B*)-stained sections from the right hemisphere of a monocularly deprived animal's LGN. In both panels, the *top* of the figure is dorsal, and the *right* side is medial. Scale bars = 1 mm.

### *Qualitative physiological observations*

We determined the laminar location of each neuron, usually from the stereotypic shift in ocular dominance of the receptive fields as our electrode traversed vertically through each of the six geniculate laminae. We confirmed our assessments of laminar location histologically (see METHODS). Our normal sample includes 94 neurons in magnocellular laminae 1 and 2, plus 120 in parvocellular laminae 3–6; our sample from the monocularly deprived animals consists of 62 deprived parvocellular neurons, 75 nondeprived parvocellular neurons (including 4 binocular cells between parvocellular laminae), 56 deprived magnocellular neurons, and 61 nondeprived magnocellular neurons.

Table 1 shows our sample of recorded units from the monocularly deprived animals. In testing cells in laminae con-

TABLE 1. *Distribution of units recorded in the LGN of animals deprived of vision in the right eye from birth to the age of 5–6 yr*

| | Magnocellular | Parvocellular |
|---|---|---|
| LGN contralateral to deprived eye | | |
| Deprived eye | 28 | 32 |
| Nondeprived eye | 30 | 37 |
| LGN ipsilateral to deprived eye | | |
| Deprived eye | 28 | 30 |
| Nondeprived eye | 31 | 34 |

LGN, lateral geniculate nucleus.

nected to the deprived and nondeprived eyes, we were careful to sample equally from the LGNs both contra- *and* ipsilateral to the deprived eye. We recorded in the same range of eccentricities as in the normal animals; as in the normals, we also took pains to obtain our magno- and parvocellular samples at similar retinal eccentricities (see following text). Although we sampled the LGN ipsilateral to the deprived eye (i.e., the right hemisphere) at slightly more peripheral eccentricities, we found no consistent differences in response properties between the hemispheres in the deprived animals (see Table 4) and have therefore pooled data across hemispheres.

CELL TYPES. Our distribution of geniculate neurons sensitive to chromatic (types I, II, and IV) and luminance (type III) contrast agrees well with that originally described by Wiesel and Hubel (1966). In the normal animals, we found that only one magnocellular neuron (1%) was chromatically opponent and that a substantial minority of 44 parvocellular neurons (40%) were type III. However, as Derrington et al. (1984) noted, it seems likely that nearly every parvocellular neuron exhibits some degree of chromatic opponency, a phenomenon that our techniques were probably too crude to demonstrate. The proportions of the various cell types encountered in the deprived animals did not seem to differ either from the normal animals or between deprived and nondeprived laminae. In deprived magnocellular laminae, 1 cell in 57 (1.8%) was chromatically opponent versus 3% (3/61) of the nondeprived magnocellular neurons. In deprived parvocellular laminae, 14.5% (9/62) of the sample was type III, while 20% (15/74) of the nondeprived sample was.

ECCENTRICITY. The receptive field eccentricities of our normal parvocellular sample ranged from 0 to 9°, while those of our normal magnocellular sample ranged from 0 to 14°. A substantial proportion of both magno- and parvocellular samples was within the central 5°; however, while essentially the entire parvocellular sample (94%) was within the central 5°, only about half of the magnocellular sample was. We therefore also list in Table 3 summary statistics of our magno- and parvocellular samples restricted to the central 5°. More detailed descriptions of eccentricity values of our neuronal sample are given in the following text in relationship to other variables. Where response characteristics vary with eccentricity we make comparisons between magno- and parvocellular samples restricted to this matched range of eccentricities. In the monocularly deprived animals, all LGN divisions (deprived and nondeprived magno- and parvocellular) were sampled at similar eccentricities (i.e., from 0 to 8°, mean eccentricity of roughly 4°).

DISTRIBUTION OF ON- AND OFF-CENTER CELLS. Table 2 shows the distribution of on- and off-center cells across the laminae for our normal and deprived animal samples. In the normal animals, we observed an obvious center/surround organization in 207 (96.7%) of the receptive fields. There were clear interlaminar differences among these in the balance of on- and off-center cells. Although we found an approximate balance for the entire normal sample (106 on center vs. 101 off center), the parvocellular sample contained mostly on-center cells (70 on center vs. 46 off center), while the magnocellular sample was dominated by off-center cells (36 on center vs. 55 off center), and the anisometry of distribution is statistically significant ($P < 0.01$ on a $\chi^2$ test). We did not observe the dramatic segregation of on- and off-center cells for the parvocellular laminae as described by Schiller and Malpeli (1978), who concluded that laminae 5 and 6 were nearly exclusively on center and laminae 3 and 4 off center (see also Derrington and Lennie 1984). As shown in Table 2, however, we did observe a preponderance of on-center cells in both laminae 5 and 6 (and this held in each of the monkeys); curiously, in each monkey we also encountered more off-center cells in lamina 1.

We observed a broadly similar pattern in both deprived and nondeprived laminae of the monocularly deprived animals, although there were certain differences. In contrast to the approximate balance between on- and off-center cells seen in the normal animals' LGN, there were clearly more on- than off-center cells in total in the deprived animals' LGN, and the parvocellular laminae were again dominated by on-center cells. The overall anisometry of distribution of on- and off-center cells was significant as in the normal animals ($P < 0.005$ in deprived-eye laminae, $P < 0.01$ in nondeprived-eye laminae). However, the preponderance of on-center cells in laminae 5 and 6 was more pronounced and the preponderance of off-center cells in laminae 1 and 2 was less pronounced than in the normal animals. While such differences could conceivably result from sampling biases, they might also reflect subtle species differences between the normal animals (*M. fascicu-*

TABLE 2. *Distribution of on- and off-center cells in different layers of the LGN*

| Layer | Neurons | Percent On | Percent Off |
|---|---|---|---|
| Normal animals | | | |
| 1 | 53 | 37.7 | 62.3 |
| 2 | 38 | 42.1 | 57.9 |
| 3 | 26 | 42.3 | 57.7 |
| 4 | 33 | 54.5 | 45.5 |
| 5 | 32 | 68.8 | 31.3 |
| 6 | 25 | 76.0 | 24.0 |
| Total | 207 | 51.2 | 48.8 |
| Monocularly deprived animals | | | |
| Deprived-eye layers | | | |
| 1 | 28 | 50.0 | 50.0 |
| 2 | 28 | 42.9 | 57.1 |
| 3 | 19 | 42.1 | 57.9 |
| 4 | 10 | 60.0 | 40.0 |
| 5 | 10 | 100.0 | 0.0 |
| 6 | 22 | 77.3 | 22.7 |
| Total | 116 | 59.5 | 40.5 |
| Nondeprived-eye layers | | | |
| 1 | 29 | 58.6 | 41.4 |
| 2 | 29 | 48.3 | 51.7 |
| 3 | 18 | 55.6 | 44.4 |
| 4 | 9 | 33.3 | 66.7 |
| 5 | 19 | 73.7 | 26.3 |
| 6 | 24 | 95.8 | 4.2 |
| Total | 128 | 63.3 | 36.7 |

*laris*) and the deprived animals (*M. mulatta*). In any case, deprivation had no obvious effect on the relative proportions or distribution across laminae of on- and off-center cells.

### *Quantitative physiological observations*

LATENCY TO OPTIC CHIASM STIMULATION. Figure 2 shows that for the 203 normal LGN neurons from which we obtained a measure of the response latency to activation of the optic chiasm (OX), cells in the magnocellular laminae exhibited significantly shorter latencies than did parvocellular cells, and this difference was seen for each of the four monkeys (parvocellular: 3.14 ± 0.54 ms, magnocellular: 1.76 ± 0.33 ms; $P < 0.001$ on a Mann-Whitney $U$ test for each monkey). This confirms earlier observations (Dreher et al. 1976; Kaplan and Shapley 1982; Marrocco et al. 1982). We found no difference in this parameter between parvocellular neurons identified as types I, II, or IV and those identified as type III, which indicates that this aspect of receptive field organization is not correlated with the conduction velocity of the retinogeniculate input. Finally, we found no relationship between OX latency and receptive field eccentricity for either magno- or parvocellular neurons. OX latencies in the monocularly deprived animals differed between magno- and parvocellular groups as in the normals and did not differ significantly between the deprived and nondeprived parvocellular samples (deprived: 3.20 ± 0.51 ms, nondeprived: 3.19 ± 0.46 ms). There was a small but statistically reliable difference between deprived and nondeprived magnocellular neurons (deprived: 1.72 ± 0.32 ms, nondeprived: 1.86 ± 0.26 ms, $P < 0.018$); the significance of this observation is unclear.

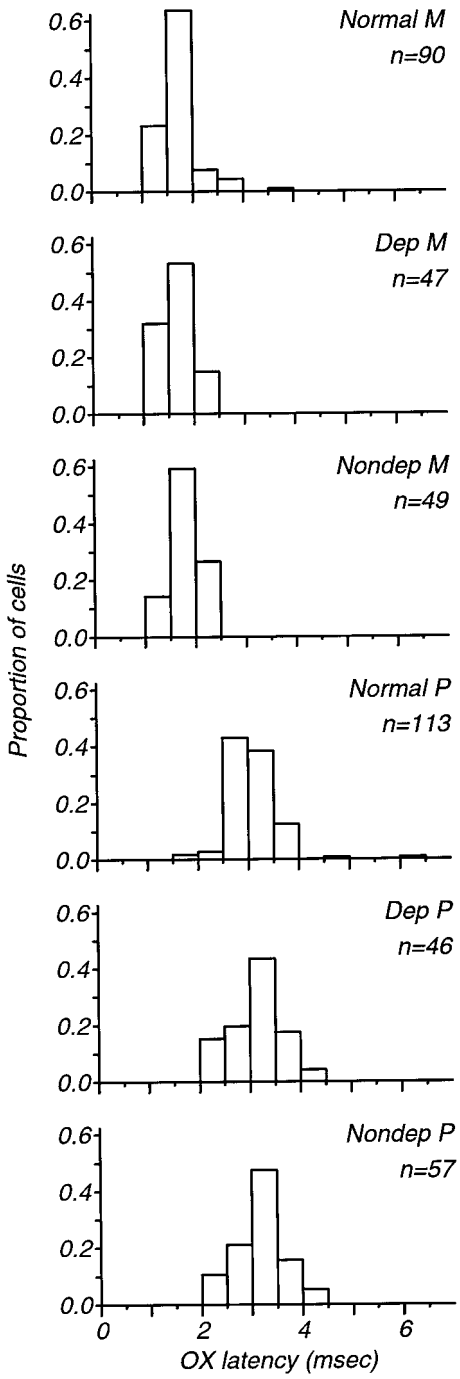


FIG. 2. Distributions of lateral geniculate nucleus (LGN) response latencies (in ms) following electrical stimulation of the optic chiasm. Shown separately (and in succeeding figures) are normal (Normal M), deprived (Dep M), and nondeprived (Nondep M) magnocellular neurons, and normal (Normal P), deprived (Dep P), and nondeprived (Nondep P) parvocellular neurons.

Save for the differences in laminar distributions of on- and off-center receptive fields noted in the preceding text, the magno- and parvocellular populations each appeared to be fairly homogeneous and quite distinct from one another. Thus in the quantitative analyses in the following text, data from these various cell types will generally be pooled across the magno- or parvocellular laminae. We used a consistent protocol to study the responses of each neuron, yielding the set of measurements shown in Fig. 3 for a single magnocellular neuron.

First, we determined spatial properties of neurons with drifting and counterphase flickered gratings. These gratings had a contrast of 0.5 and a temporal frequency of 4 Hz. For the drifting gratings (Fig. 3*A*), six spatial frequencies from 0.38 to 12 c/° in octave steps were chosen; zero spatial frequency (or DC) was approximated by sinusoidally flickering a blank screen at 4 Hz and at a depth of modulation equivalent to the luminance difference between the brightest and darkest points along the gratings. The counterphase flickered gratings had the same range of spatial frequencies; for each frequency, we presented these at six equally spaced absolute spatial phases.

We found no substantive or consistent differences between the tuning functions taken from drifting gratings and those derived from counterphased flickering gratings. We therefore took most spatial properties of these neurons from the modulated responses to drifting gratings. We used the difference of Gaussians receptive field model to derive a number of spatial properties from the tuning curve (Derrington and Lennie 1984; Enroth-Cugell and Robson 1966; Rodieck 1965). To each spatial frequency response, we fit a function (Fig. 3*A*, —) of the form

$$R = k(\exp(-(f/f_c)^2) - k_s \exp(-(f/f_s)^2))$$

where $R$ is response, $k$ is an overall scaling factor, $k_s$ is the relative strength of the surround, and $f_c$ and $f_s$ are the characteristic spatial frequencies of the center and surround mechanisms. From these characteristic frequencies, we calculated the characteristic radii of the center and surround mechanisms (Enroth-Cugell and Robson 1966).

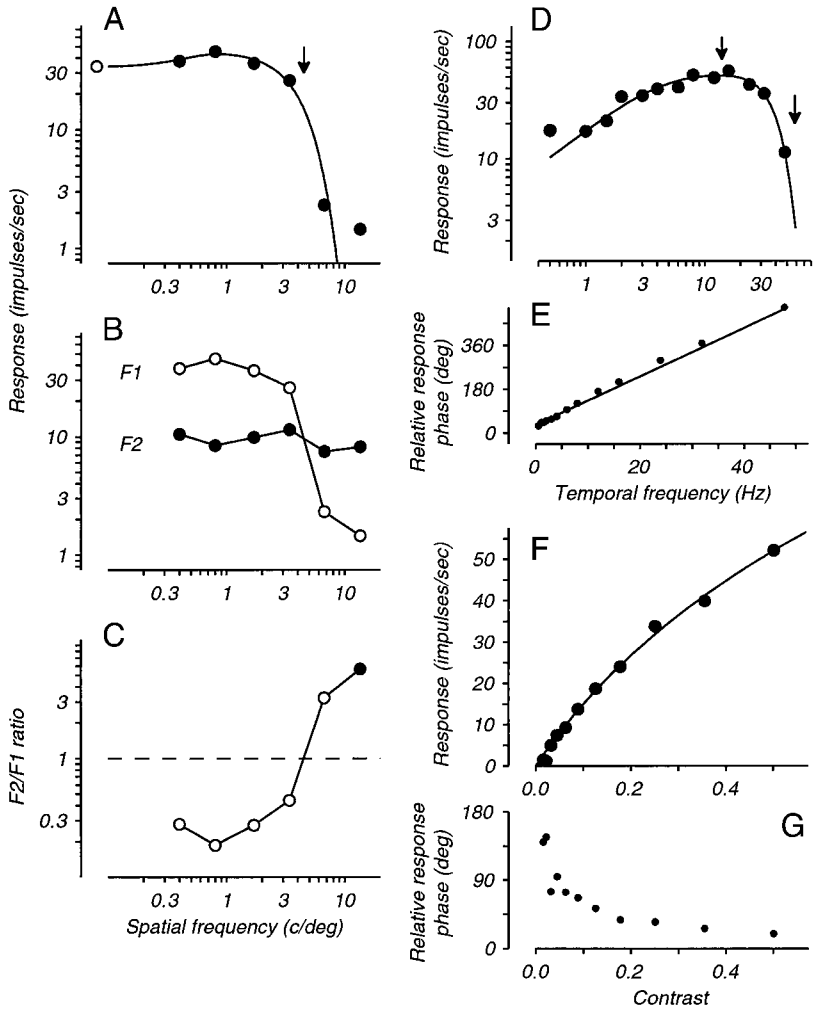


FIG. 3. Response measures derived from a single representative magnocellular LGN cell. In all panels, F1 response (see METHODS) is used unless otherwise noted. *A*: spatial frequency response function: ●, drifting gratings; ○, uniform field flicker. —, the best-fitting difference-of-Gaussians function; ↓, center characteristic spatial frequency ( $f_c$). *B*: amplitude of F1 (○) and mean F2 responses (●), and their ratio (*C*) as a function of spatial frequency. ● in *C* indicates an undefined ratio as F1 response was indistinguishable from baseline at this spatial frequency. *D*: temporal frequency response function. —, the best-fitting difference-of-exponentials function. ↓, optimal temporal frequency and temporal resolution. *E*: response temporal phase as a function of stimulus temporal frequency. *F* and *G*: response amplitude and response temporal phase, respectively, as a function of stimulus contrast. — in *F* is best-fitting saturating function.

The counterphase flickered gratings were used to test the linearity of each cell's spatial summation by examining the fundamental (F1) and second harmonic (F2) response components. The F1 response varies sinusoidally with the spatial phase of the grating, whereas the F2 response is for the most part independent of spatial phase. At each spatial frequency where there was a reliable evoked response, we calculated the ratio of the mean of the F2 responses to the amplitude of the F1 responses (Fig. 3, *B* and *C*). The maximum value of this ratio across spatial frequency we define as the "nonlinearity index," closely following Shapley and Hochstein (1975) and Hochstein and Shapley (1976).

Second, we determined the temporal properties of each cell by measuring responses to gratings of 0.5 contrast and optimal spatial frequency, drifted at 7–13 different temporal frequencies (Fig. 3*D*). These were varied in octave or half-octave steps from 0.5 to 48 Hz. To the temporal frequency response data, we fitted a function representing cascaded low-pass exponential and high-pass RC filters (Fig. 3*D*, —) and from the fit determined each cell's optimal temporal frequency (peak response), temporal resolution (high temporal frequency at half-maximum response), and response transience (the slope of the low frequency limb of the function, see following text). Since the temporal phase of each neuron's response to different temporal frequencies was proportional to temporal frequency, the slope of the resulting line is the "steady-state visual latency," which provides a measure of each neuron's temporal integration behavior (Fig. 3*E*).

Third, we studied response as a function of stimulus contrast, using gratings of optimal spatial frequency. We chose a temporal frequency at or slightly below the optimum to take account of contrast gain control effects (Shapley and Victor 1978). The contrast of these gratings usually ranged from 0.015 to 0.7 in steps of 0.15 log units (Fig. 3*F*). To these data, we fit the function suggested by Robson (1975)

$$R = k \log\left(1 + \frac{C}{C_0}\right)$$

where $R$ is response, $k$ is a scaling factor, $C$ is contrast, and $C_0$ is a saturation constant. Over the range of contrasts we used, parvocellular responses were nearly linear, but magnocellular responses often showed a nonlinear saturation at higher contrasts. At low contrasts, however, all cells gave responses proportional to contrast; the slope of the contrast response function at 0 contrast, $k/C_0$, is our measure of responsivity. We also determined the degree to which the temporal phase of responses depended on stimulus contrast [indicative of the contrast gain control described by Shapley and Victor (1978)] (Fig. 3*G*). We fitted a function simultaneously to both the amplitude and phase of contrast response data (Carandini et al. 1997), and from this complex function we extracted a function relating temporal response phase to stimulus contrast. From

this phase versus contrast function, we determined the difference in response phase between the 50% contrast condition and the blank condition (0% contrast); we took this "phase advance," expressed in milliseconds, to measure contrast gain control.

Tables 3 and 4 summarize a number of the parameters that we determined quantitatively for neurons in the normal and monocularly deprived animals. These are shown separately for magno- and parvocellular neurons. The parameters shown, defined in the preceding text and considered in more detail in the following text (see also DISCUSSION), include receptive field eccentricity in deg, response latency to optic chiasm stimulation in seconds (OX latency), radius in degrees ($r_c$), and characteristic frequency in c/degree ($f_c$) of the center mechanism, surround sensitivity ($k_s$), nonlinearity, optimal and cutoff temporal frequencies in Hz, response latency to visual stimuli in milliseconds (visual latency), response transience, responsivity, and phase advance in milliseconds.

SPATIAL PROPERTIES. Figure 4 illustrates the distributions of the characteristic frequencies ($f_c$) of our magno- and parvocellular samples (derived from spatial tuning functions as described in the preceding text), and Fig. 5 shows the variations of $f_c$ and $r_c$ (center radius) with eccentricity. Note that, with increasing eccentricity, $r_c$ increases and $f_c$ decreases, although this trend was somewhat less obvious in the monocularly deprived animals (due to the presence in these animals of units with lower spatial resolutions close to the fovea and with higher spatial resolutions at intermediate eccentricities). This again might reflect subtle species differences. However, Derrington and Lennie (1984) and Spear et al. (1994) observed a similar weak dependence on eccentricity of these parameters within the central 10° in both *M. mulatta* and *M. fascicularis* monkeys. Note also that with our methodology, we found little difference between magno- and parvocellular neurons, in both normal and deprived animals, with respect to these variables. This belies the expectation that magnocellular neurons should have markedly larger $r_c$ values and poorer resolution than parvocellular neurons at matched eccentricities (Derrington and Lennie 1984; Kaplan and Shapley 1982; Merigan et al. 1991) but is in accord with the findings of Spear et al. (1994). Our normal sample with receptive fields within 1° of the fovea is predominantly parvocellular, and beyond 8° it is exclusively magnocellular. Although parvocellular neurons on average had somewhat larger $f_c$ and smaller $r_c$ values ($f_c$: parvocellular, 4.57 ± 2.73 c/° and magnocellular, 2.82 ± 1.68 c/°; $r_c$: parvocellular, 0.069 ± 0.076° and magnocellular, 0.112 ± 0.080°), this partially reflects the eccentricity differences in our normal samples. In our samples within both the 1–2.5° and 3–7.5° sectors of reasonably matched eccentricity, we found no significant differences between parvo- and magnocellular neurons for mean or variance of $r_c$ and $f_c$ values. In our sample restricted to the central 5°, we did still find a small (though significant) difference between parvo- and magnocellular neurons ($f_c$: parvocellular, 4.57 ± 2.75 c/°; magnocellular, 3.55 ± 1.94 c/°; $P < 0.02$). This is consistent with the results of Spear et al. (1994) and of Blakemore and Vital-Durand (1986a), who found that the majority of parvo- and magnocellular neurons at a given eccentricity (the X-like ones) had similar spatial resolution. However, we have noted, as have Derrington and Lennie (1984) and Spear et al. (1994), that the smallest $r_c$ (and highest $f_c$ and spatial resolution values) at each eccentricity tend to belong to the parvocellular cells. The values of $f_c$ and $r_c$ in the deprived animals did not differ significantly from those values in the normal animals, nor did we find any effect of deprivation.

We found no significant differences between the parvo- and magnocellular populations in the mean strength of receptive field surrounds ($k_s$: parvocellular, 0.54 ± 0.35; magnocellular, 0.60 ± 0.33), nor did this parameter vary significantly with eccentricity. Deprivation had no effect on $k_s$ for parvocellular neurons, but the relative strength of the surround mechanism was stronger in magnocellular neurons in deprived-eye laminae than in nondeprived laminae (deprived, 0.60 ± 0.18; nondeprived, 0.41 ± 0.24; $P < 0.0035$).

Figure 6 summarizes the distribution of nonlinearity index values. Larger values indicate greater frequency-doubled responses relative to the F1 component, indicative of nonlinearities in spatial summation, i.e., "Y-like" behavior. We found no

TABLE 3. *Summary statistics for 214 neurons recorded from 4 normal monkeys*

| | RF Eccentricity, ° | OX Latency, ms | $f_c$, C/° | $r_c$, ° | $k_s$ | Optimal TF, Hz | Cutoff TF, Hz | Visual Latency, ms | Transience | Responsivity, imp · $s^{-1}$ · $contrast^{-1}$ | Nonlinearity | Phase Advance, ms |
|---|---|---|---|---|---|---|---|---|---|---|---|---|
| Magnocellular neurons (94) | | | | | | | | | | | | |
| *n* | 91 | 90 | 75 | 75 | 75 | 59 | 59 | 59 | 59 | 55 | 75 | 55 |
| Mean | 5.73 ± 3.36 | 1.76 ± 0.33 | 2.82 ± 1.68 | 0.112 ± 0.080 | 0.60 ± 0.33 | 7.94 ± 4.80 | 31.62 ± 15.85 | 37.91 ± 4.51 | 0.54 ± 0.29 | 87.10 ± 80.08 | 0.65 ± 0.55 | 17.70 ± 10.42 |
| Parvocellular neurons (120) | | | | | | | | | | | | |
| *n* | 116 | 113 | 84 | 84 | 84 | 70 | 70 | 70 | 70 | 64 | 84 | 64 |
| Mean | 2.52 ± 1.66 | 3.14 ± 0.54 | 4.57 ± 2.73 | 0.069 ± 0.076 | 0.54 ± 0.35 | 6.76 ± 3.24 | 21.88 ± 12.30 | 44.81 ± 8.27 | 0.70 ± 0.41 | 23.44 ± 24.22 | 0.42 ± 0.19 | 6.69 ± 8.02 |
| Magnocellular neurons in central 5° (43) | | | | | | | | | | | | |
| *n* | 43 | 42 | 33 | 33 | 33 | 28 | 28 | 28 | 28 | 25 | 33 | 25 |
| Mean | 2.71 ± 1.37 | 1.70 ± 0.35 | 3.55 ± 1.94 | 0.089 ± 0.070 | 0.68 ± 0.37 | 7.59 ± 4.67 | 27.54 ± 13.67 | 38.99 ± 3.53 | 0.61 ± 0.29 | 91.20 ± 76.81 | 0.63 ± 0.52 | 18.39 ± 8.58 |
| Parvocellular neurons in central 5° (110) | | | | | | | | | | | | |
| *n* | 110 | 106 | 82 | 82 | 82 | 68 | 68 | 68 | 68 | 62 | 82 | 62 |
| Mean | 2.24 ± 1.13 | 3.14 ± 0.55 | 4.57 ± 2.75 | 0.069 ± 0.076 | 0.52 ± 0.35 | 6.76 ± 3.28 | 21.38 ± 11.67 | 44.90 ± 8.37 | 0.71 ± 0.41 | 23.44 ± 24.56 | 0.42 ± 0.19 | 6.58 ± 8.03 |

Parameters listed are: receptive field eccentricity, OX latency (response latency to optic chiasm stimulation), $f_c$ (receptive field center frequency), $r_c$ (receptive field center radius), $k_s$ (relative strength of surround mechanism), nonlinearity index, optimal and cutoff temporal frequencies, visual response latency, transience index, responsivity, and phase advance. Number of cells recorded (*n*), mean value and standard deviation (SD) are listed for each parameter. Geometric means reported for $f_c$, $r_c$, $k_s$, nonlinearity, TF optima, and cutoffs. Arithmetic means reported for eccentricity, OX latency, visual latency, transience, and phase advance. Values calculated separately for the entire LGN sample, entire magno- and parvocellular samples, and samples restricted to the central 5°.

TABLE 4. *Summary statistics for 254 neurons recorded from 5 monocularly deprived monkeys*

| | RF Eccentricity, ° | OX Latency, ms | $f_c$, C/° | $r_c$, ° | $k_s$ |
|---|---|---|---|---|---|
| *Parvocellular neurons, deprived-eye layers* (all cells = 62) | | | | | |
| *n* | 61 | 46 | 54 | 54 | 54 |
| Mean | 4.00 ± 2.33 | 3.20 ± 0.51 | 4.79 ± 3.51 | 0.066 ± 0.077 | 0.46 ± 0.24 |
| Ipsilateral to deprived eye (30) | | | | | |
| *n* | 29 | 22 | 26 | 26 | 26 |
| Mean | 5.28 ± 2.23 | 3.22 ± 0.44 | 3.89 ± 2.77 | 0.081 ± 0.060 | 0.40 ± 0.29 |
| Contralateral to deprived eye (32) | | | | | |
| *n* | 32 | 24 | 28 | 28 | 28 |
| Mean | 2.84 ± 1.74 | 3.18 ± 0.56 | 5.89 ± 3.71 | 0.055 ± 0.089 | 0.52 ± 0.19 |
| *Magnocellular neurons, deprived-eye layers* (all cells = 56) | | | | | |
| *n* | 56 | 47 | 52 | 52 | 52 |
| Mean | 4.41 ± 2.86 | 1.72 ± 0.32 | 3.55 ± 1.30 | 0.089 ± 0.037 | 0.60 ± 0.18 |
| Ipsilateral to deprived eye (28) | | | | | |
| *n* | 28 | 26 | 27 | 27 | 27 |
| Mean | 6.54 ± 2.46 | 1.70 ± 0.31 | 3.55 ± 1.22 | 0.089 ± 0.035 | 0.60 ± 0.21 |
| Contralateral to deprived eye (28) | | | | | |
| *n* | 28 | 21 | 25 | 25 | 25 |
| Mean | 2.27 ± 1.05 | 1.75 ± 0.32 | 3.55 ± 1.37 | 0.089 ± 0.040 | 0.59 ± 0.14 |
| *Parvocellular neurons, nondeprived-eye layers* (all cells = 75, including 4 binocular) | | | | | |
| *n* | 70 | 57 | 64 | 64 | 64 |
| Mean | 3.14 ± 2.20 | 3.19 ± 0.46 | 3.63 ± 3.91 | 0.087 ± 0.146 | 0.50 ± 0.24 |
| Ipsilateral to deprived eye (37) | | | | | |
| *n* | 37 | 30 | 35 | 35 | 35 |
| Mean | 1.62 ± 0.64 | 3.08 ± 0.51 | 3.02 ± 3.33 | 0.107 ± 0.146 | 0.51 ± 0.23 |
| Contralateral to deprived eye (34) | | | | | |
| *n* | 31 | 24 | 28 | 28 | 28 |
| Mean | 5.08 ± 1.91 | 3.30 ± 0.37 | 4.79 ± 4.23 | 0.066 ± 0.136 | 0.47 ± 0.25 |
| *Magnocellular neurons, nondeprived-eye layers* (all cells = 61) | | | | | |
| *n* | 61 | 58 | 58 | 58 | 58 |
| Mean | 4.05 ± 2.99 | 1.86 ± 0.26 | 3.24 ± 2.31 | 0.098 ± 0.084 | 0.41 ± 0.24 |
| Ipsilateral to deprived eye (30) | | | | | |
| *n* | 30 | 19 | 30 | 30 | 30 |
| Mean | 2.36 ± 0.88 | 1.78 ± 0.28 | 2.51 ± 1.78 | 0.126 ± 0.080 | 0.36 ± 0.19 |
| Contralateral to deprived eye (31) | | | | | |
| *n* | 31 | 30 | 28 | 28 | 28 |
| Mean | 5.69 ± 3.37 | 1.92 ± 0.23 | 4.17 ± 2.43 | 0.076 ± 0.077 | 0.47 ± 0.25 |

change in this index with eccentricity for either the magno- or parvocellular populations. On average, magnocellular neurons display greater nonlinearity indices than do parvocellular neurons, consistent with previous reports that the nonlinear (Y-like) cells are found as a subgroup only within the magnocellular laminae (parvocellular, 0.42 ± 0.19; magnocellular, 0.65 ± 0.55); this difference was significant in both the overall sample and the sample restricted to the central 5° ($P < 0.001$). However, there is considerable overlap between populations, and both the parvo- and magnocellular distributions are essentially unimodal, an observation in agreement with that of Derrington and Lennie (1984).

Comparison between deprived and nondeprived laminae suggests that there was a small but significant decrease in the average nonlinearity indices of our monocularly deprived sample in both magno- and parvocellular laminae (parvocellular nondeprived, 0.47 ± 0.20; parvocellular deprived, 0.38 ± 0.16, $P < 0.0085$; magnocellular nondeprived, 0.56 ± 0.28; magnocelluar deprived, 0.42 ± 0.31, $P < 0.0006$). Although this is reminiscent of the Y-cell loss noted in cats following monocular deprivation (Sherman et al. 1972; but see So and Shapley 1980), the effect is not the same. Here, we see a decrease in nonlinearity indices in *both* magno- and parvocellular laminae, while only the magnocellular laminae contain the nonlinear (Y-like) cells, i.e., those with indices greater than 1 (Blakemore and Vital-Durand 1986a; Kaplan and Shapley 1982). Furthermore we found no evidence for the loss of any one subpopulation; nonlinear cells were still found in deprived laminae. Rather, we observed a simple shift in the overall population distributions that was approximately 0.5 of a standard deviation in both magno- and parvocellular layers.

The unimodal distributions of nonlinearity index shown in Fig. 6 do not by themselves rule out the suggestion of Kaplan and Shapley (1982) that magnocellular neurons can be classified into distinct linear (X) and nonlinear (Y) types, since these types might differ both in their linearity and in such other characteristics as their spatial resolution or the conduction velocity of their retinal afferents. Figure 7*A* shows scatter plots, separately for magno- and parvocellular neurons, of characteristic frequency ($f_c$, equivalently center radius $r_c$, right-hand ordinate) versus nonlinearity index for our normal sample (Fig. 7*A*, *left*) and for our deprived sample (*right*), which again shows that both these parameters were continuously distributed with no clear segregation into subpopulations. Inspection of the

TABLE 4. *(continued)*

| Optimal TF, Hz | Cutoff TF, Hz | Visual Latency, ms | Transience | Responsivity, imp · $s^{-1}$ · $contrast^{-1}$ | Nonlinearity | Phase Advance, ms |
|---|---|---|---|---|---|---|
| 52<br>7.41 ± 5.01 | 52<br>20.89 ± 10.94 | 43<br>54.58 ± 49.42 | 52<br>0.60 ± 0.48 | 47<br>26.30 ± 105.24 | 48<br>0.38 ± 0.16 | 45<br>8.31 ± 12.89 |
| 23<br>7.08 ± 6.85 | 23<br>23.44 ± 13.67 | 20<br>68.02 ± 69.83 | 23<br>0.61 ± 0.52 | 20<br>37.15 ± 152.90 | 20<br>0.43 ± 0.17 | 19<br>8.91 ± 14.43 |
| 29<br>7.59 ± 2.70 | 29<br>19.05 ± 7.06 | 23<br>42.90 ± 5.64 | 29<br>0.60 ± 0.44 | 27<br>20.42 ± 29.13 | 28<br>0.35 ± 0.15 | 26<br>7.86 ± 11.61 |
| 47<br>10.47 ± 4.43 | 47<br>26.92 ± 8.74 | 45<br>41.06 ± 11.67 | 47<br>0.47 ± 0.28 | 45<br>177.83 ± 285.49 | 52<br>0.42 ± 0.31 | 43<br>17.43 ± 10.86 |
| 25<br>9.12 ± 4.61 | 25<br>23.99 ± 9.94 | 25<br>39.58 ± 6.36 | 25<br>0.54 ± 0.31 | 23<br>134.90 ± 218.69 | 27<br>0.39 ± 0.22 | 22<br>16.08 ± 12.38 |
| 22<br>12.02 ± 3.92 | 22<br>30.20 ± 6.21 | 20<br>42.90 ± 15.80 | 22<br>0.40 ± 0.21 | 22<br>234.42 ± 334.95 | 25<br>0.45 ± 0.38 | 21<br>18.85 ± 8.79 |
| 55<br>7.59 ± 4.20 | 55<br>21.38 ± 10.49 | 47<br>46.96 ± 21.45 | 55<br>0.62 ± 0.41 | 52<br>33.16 ± 114.59 | 57<br>0.47 ± 0.20 | 52<br>10.24 ± 14.87 |
| 32<br>7.59 ± 3.95 | 32<br>22.91 ± 11.24 | 27<br>50.56 ± 11.24 | 32<br>0.63 ± 0.36 | 30<br>35.48 ± 141.65 | 32<br>0.45 ± 0.20 | 30<br>14.37 ± 17.69 |
| 22<br>7.76 ± 4.53 | 22<br>20.42 ± 8.53 | 20<br>42.09 ± 21.04 | 22<br>0.62 ± 0.47 | 21<br>31.62 ± 50.21 | 24<br>0.50 ± 0.20 | 21<br>3.99 ± 5.90 |
| 57<br>8.51 ± 5.48 | 57<br>26.30 ± 12.35 | 54<br>40.90 ± 7.51 | 57<br>0.47 ± 0.29 | 56<br>251.19 ± 341.45 | 58<br>0.56 ± 0.28 | 53<br>20.72 ± 12.15 |
| 30<br>6.76 ± 5.31 | 30<br>22.91 ± 12.99 | 30<br>42.97 ± 8.24 | 30<br>0.57 ± 0.33 | 30<br>204.17 ± 220.47 | 30<br>0.54 ± 0.26 | 28<br>20.50 ± 13.73 |
| 27<br>10.96 ± 4.88 | 27<br>31.62 ± 10.14 | 24<br>38.32 ± 5.47 | 27<br>0.35 ± 0.16 | 26<br>323.59 ± 412.91 | 28<br>0.59 ± 0.30 | 25<br>20.97 ± 10.09 |

data from deprived animals reveals no evidence of a loss of a particular cell group; data from deprived laminae are simply shifted toward lower values of the nonlinearity index (cf. Fig. 6). Figure 7*B* shows similar plots of OX response latency versus nonlinearity index. There is again no evidence for a distinctive group of nonlinear neurons in either population, nor do similar displays (not shown) of nonlinearity index against other properties such as spatial or temporal resolution reveal subgroups. These results therefore do not support earlier suggestions that there are separate X and Y cells in the magnocellular layers; rather, the magno- and parvocellular layers each seem to contain a single class of neuron with some diversity of properties within the class.

TEMPORAL PROPERTIES. Figure 8 illustrates the distributions of our observed temporal resolution values. As noted in the preceding text, the optimum spatial frequency and spatial resolution were also determined for these neurons, but we found no correlation between these spatial and temporal variables. There was no measurable influence of eccentricity on optimal temporal frequency, and we found no significant differences in temporal frequency optima between magno- and parvocellular neurons; nor did we find any significant effects of deprivation (parvocellular normal, 6.76 ± 3.24 Hz; parvocellular nondeprived, 7.59 ± 4.20 Hz; parvocellular deprived, 7.41 ± 5.01 Hz; magnocellular normal, 7.94 ± 4.80 Hz; magnocellular nondeprived, 8.51 ± 5.48 Hz; magnocellular deprived, 10.4 ± 4.4 Hz). In our normal sample, however, magnocellular neurons did on average have significantly better temporal resolution than did parvocellular neurons (parvocellular, 21.9 ± 12.3 Hz; magnocellular, 31.6 ± 15.9 Hz; $P < 0.001$). This difference might in part reflect the slight increase in temporal resolution with eccentricity ($r = 0.36$, $P < 0.01$ for magnocellular neurons; $r = 0.29$, $P < 0.05$ for parvocellular neurons) coupled with the bias in our normal magnocellular sample to more eccentric receptive field locations relative to the parvocellular sample. However, we did also observe a small significant magno-parvocellular difference in temporal resolution values in our normal sample restricted to the central 5° (parvocellular, 21.4 ± 11.7 Hz; magnocellular, 27.5 ± 13.7 Hz; $P < 0.02$).

Macaque LGN neurons have also been classified according to their capacity to maintain discharge during stimulus presentation; Dreher et al. (1976) and Schiller and Malpeli (1978) reported that responses in the parvocellular laminae are more sustained than those in the magnocellular laminae. We defined

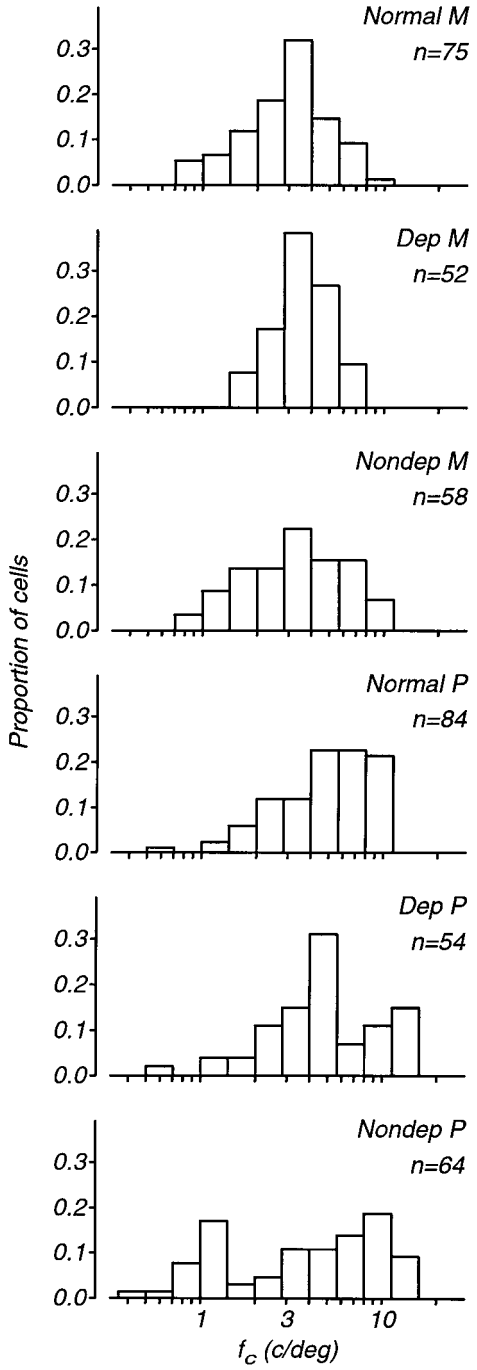


FIG. 4. Distributions of center mechanism characteristic frequencies ( $f_c$) plotted separately (as in Fig. 2) for normal, deprived, and nondeprived magno- and parvocellular neurons.

a *transience index* from each cell's temporal frequency response function by measuring the slope in log-log coordinates of the low-frequency (high-pass) limb of the function, below the optimal temporal frequency. Cells with larger transience indices had greater attenuation of responses to low temporal frequencies; this is equivalent to saying that their responses were less sustained (more transient) during stimulus presentation—assuming that neurons' temporal summation behavior is linear, which seems essentially true (Lee et al. 1994). Thus transience indices near 0 indicate perfectly low-pass temporal frequency response behavior ("sustained" responses), while larger transience indices indicate band-pass temporal frequency responses with attenuated response at low temporal frequencies ("transient" behavior). Figure 9 illustrates the distributions of transience indices of our magno- and parvocellular samples. Unexpectedly, normal magnocellular neurons on average had slightly *smaller* transience indices than normal parvocellular neurons (magnocellular, 0.54 ± 0.29; parvocellular, 0.70 ± 0.41); these distributions overlapped to a great extent and were significantly different from one another ($P < 0.0081$). The difference was not significant, however, in the samples restricted to the central 5°. This index is distributed unimodally through both magno- and parvocellular laminae with no evidence for any special subpopulations. Our finding that the distributions overlap agrees with Blakemore and Vital-Durand's (1986a) conclusion that response transience was not strongly correlated with other receptive field classification cri-

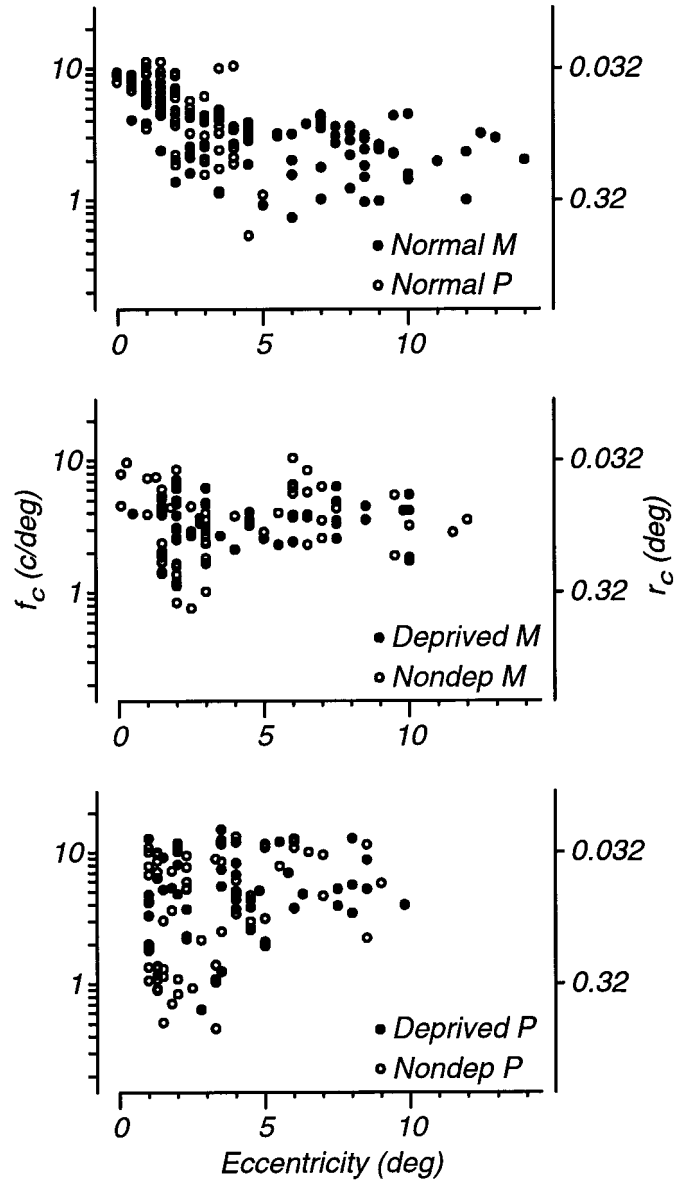


FIG. 5. Scatterplot of the relationship between center characteristic frequency $f_c$ (or receptive field center radius $r_c$) and receptive field eccentricity for normal LGN cells (*top*), deprived and nondeprived magnocellular cells (*middle*), and deprived and nondeprived parvocellular cells (*bottom*).

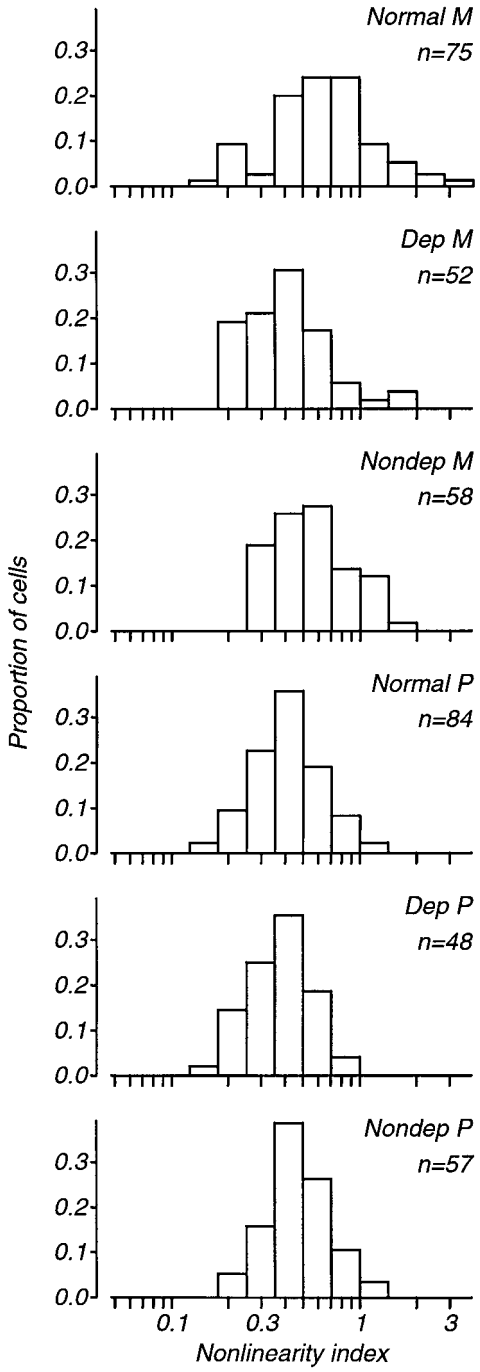


FIG. 6. Distributions of nonlinearity indices for normal, deprived, and nondeprived magno- and parvocellular neurons.

teria in macaque LGN. Our finding that parvocellular neurons were, on average, slightly *more* transient than magnocellular neurons is nonetheless unexpected.

In the monocularly deprived animals, transience indices in both parvo- and magnocellular laminae showed no significant effect of deprivation (parvocellular nondeprived, 0.62 ± 0.41; parvocellular deprived, 0.60 ± 0.48; magnocellular nondeprived, 0.47 ± 0.29; magnocellular deprived, 0.47 ± 0.28). These mean transience indices are somewhat lower than those in the normals. The differences between normal cells and either deprived or nondeprived cells were, however, significant only for the comparison of normal and deprived parvocellular neurons ($P < 0.017$). While this difference might indicate a subtle effect of deprivation on the transience of parvocellular LGN cells, the absence of a reliable difference between deprived and nondeprived cells suggests that this merely reflects minor differences between the different macaque species.

We also determined the steady-state visual response latencies for our sample. As illustrated by Fig. 10, despite substantial overlap in the distributions, magnocellular neurons' visual latencies were on average significantly shorter than those of parvocellular neurons in both normal and deprived animals, and deprivation had no significant effect on latencies (parvocellular normal, 44.8 ± 8.3 ms; magnocellular normal, 37.9 ± 4.5 ms; $P < 0.0001$; parvocellular nondeprived, 47.0 ± 21.5 ms; parvocellular deprived, 54.6 ± 49.4 ms; magnocellular nondeprived, 40.9 ± 7.5 ms; magnocellular deprived, 41.1 ± 11.7 ms). These values are significantly smaller than the mean value of approximately 77 ms reported by Spear et al. (1994). As response latency is known to vary with stimulus contrast (Sestokas and Lehmkuhle 1986; Shapley and Victor 1978), these latency differences might simply reflect differences between their experimental conditions and our own, but we are puzzled by the discrepancy. Finally, for both the magno- and parvocellular populations, we found no correlation between visual latency and receptive field eccentricity, optimum temporal frequency, or temporal resolution.

CONTRAST-RESPONSE PROPERTIES. Figure 11 shows the distributions of responsivity values in our sample and shows that for the normal magno- and parvocellular neurons we tested, magnocellular neurons were significantly more responsive than were parvocellular neurons (parvocellular, 23.4 ± 24.2; magnocellular, 87.1 ± 80.1; $P < 0.0001$). This confirms earlier observations that magnocellular neurons display greater sensitivity to luminance contrast than do parvocellular neurons (Derrington and Lennie 1984; Hicks et al. 1983; Kaplan and Shapley 1982; Schiller and Colby 1983; Spear et al. 1994). Both distributions are unimodal with no indication of distinct subpopulations in either LGN division having high or low responsivities. Nor did we find any relationship between responsivity and either receptive field eccentricity or center radius ($r_c$). In monocularly deprived animals, cells in deprived laminae had lower responsivity than those in nondeprived laminae, although this difference was significant only in the magnocellular laminae (parvocellular nondeprived, 33.1 ± 114.6; parvocellular deprived, 26.3 ± 105.2; $P > 0.05$; magnocellular nondeprived, 251.2 ± 341.5; magnocellular deprived, 177.8 ± 285.5; $P < 0.033$). We note here another likely species difference between the normals (*M. fascicularis*) and the monocularly deprived animals (*M. mulatta*); nondeprived cells in the deprived animals were more responsive than those in the normals (parvocellular normal vs. nondeprived: $P < 0.0183$; magnocellular normal vs. nondeprived: $P < 0.0001$).

Figure 12 shows the distributions of phase advance values in our magno- and parvocellular samples. It is clear that most parvocellular neurons had phase advances of less than 10 ms, whereas most magnocellular neurons had phase advance values between 10 and 40 ms, and there was no significant dependence of this parameter on eccentricity. The difference between these distributions was highly significant (parvocellular,

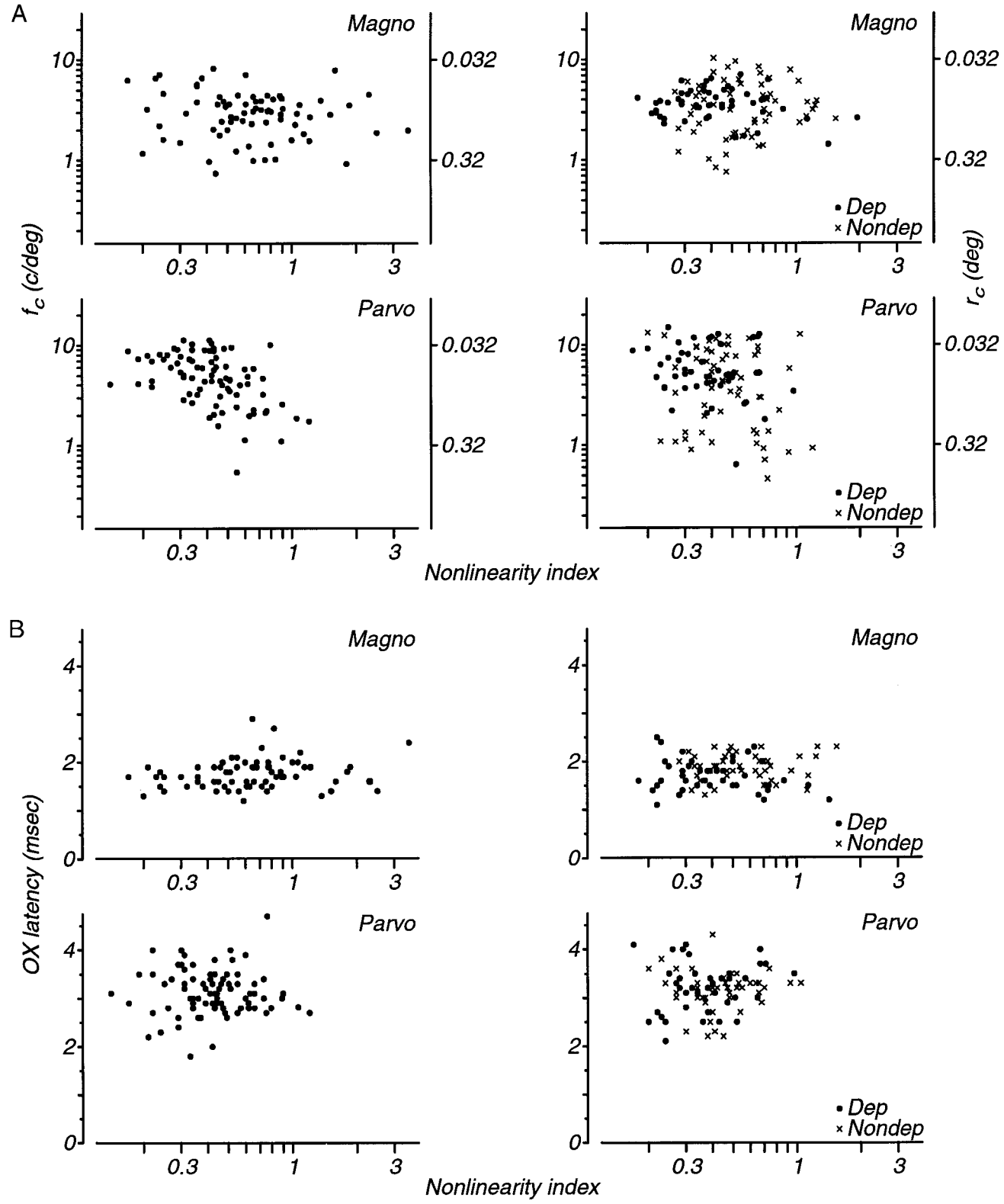


FIG. 7. *A*: scatterplots of the relationship between center characteristic frequency $f_c$ (or equivalently center radius $r_c$, right-hand ordinates) and nonlinearity index for LGN cells from normal animals (*left*) and from deprived animals (*right*). *B*: scatterplots of the relationship between latency to optic chiasm stimulation and nonlinearity index for LGN cells from normal animals (*left*) and from deprived animals (*right*). The datum from 1 parvocellular neuron from a normal animal with an optic chiasm latency of 6.4 ms has been omitted.

6.7 ± 8.0 ms; magnocellular, 17.7 ± 10.4 ms; $P < 0.0001$). This difference shows that the magnocellular laminae are distinguished not only by the presence of cells with high luminance contrast sensitivity and nonlinear spatial summation but also by cells with marked contrast gain control effects. This is again reminiscent of cat Y cells, as they are the cells exhibiting

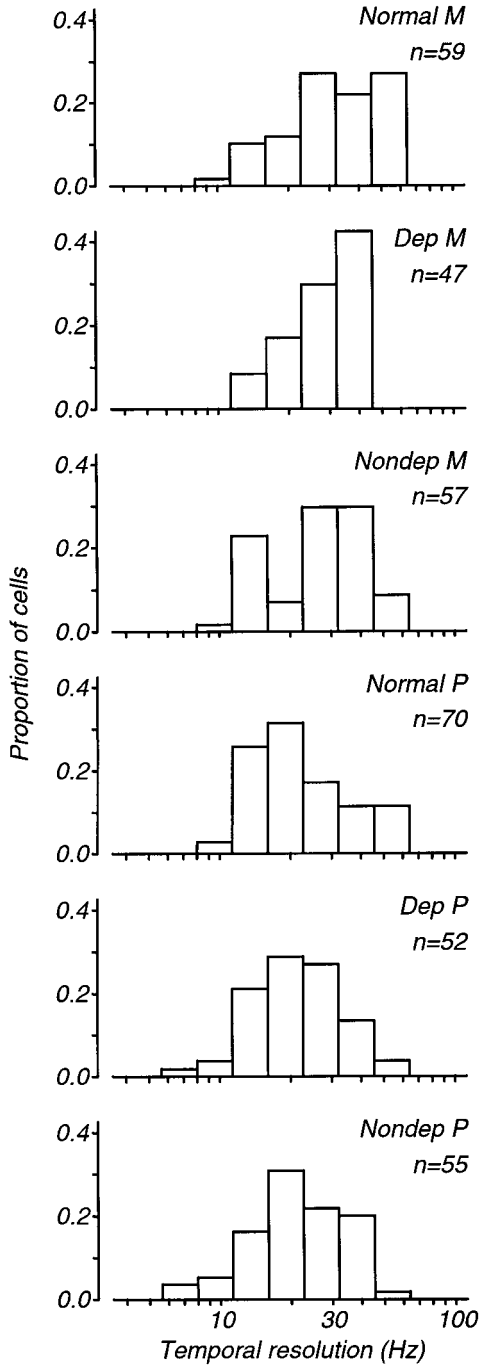


FIG. 8. Distributions of temporal resolution values (high temporal frequency at half-maximum response) for normal, deprived, and nondeprived magno- and parvocellular neurons.

such nonlinearities of spatial summation and phase advances indicative of contrast gain control (Kaplan and Shapley 1982; Shapley and Victor 1978). However, none of these attributes revealed distinct subpopulations within the macaque magnocellular laminae, as all of these parameters were unimodally distributed in our magnocellular sample, and cells showing contrast gain effects were also found (though more rarely) in the parvocellular laminae. Phase advance values differed between magno- and parvocellular laminae in the deprived animals as in the normals, and deprivation had no significant effect on the amplitude of the phase shift (parvocellular nondeprived, 10.2 ± 14.9 ms; parvocellular deprived, 8.3 ± 12.9 ms; magnocellular nondeprived, 20.7 ± 12.2 ms; magnocellular deprived, 17.4 ± 10.9 ms).

In summary, the only significant effects of monocular deprivation that we found by comparison of deprived and nondeprived laminae were the OX latency (magnocellular: deprived $<$ nondeprived, $P < 0.018$), surround strength ($k_s$) (magnocellular: deprived $>$ nondeprived, $P < 0.0035$), nonlinearity index (parvocellular: deprived $<$ nondeprived, $P < 0.0085$; magnocellular: deprived $<$ nondeprived, $P < 0.0006$),

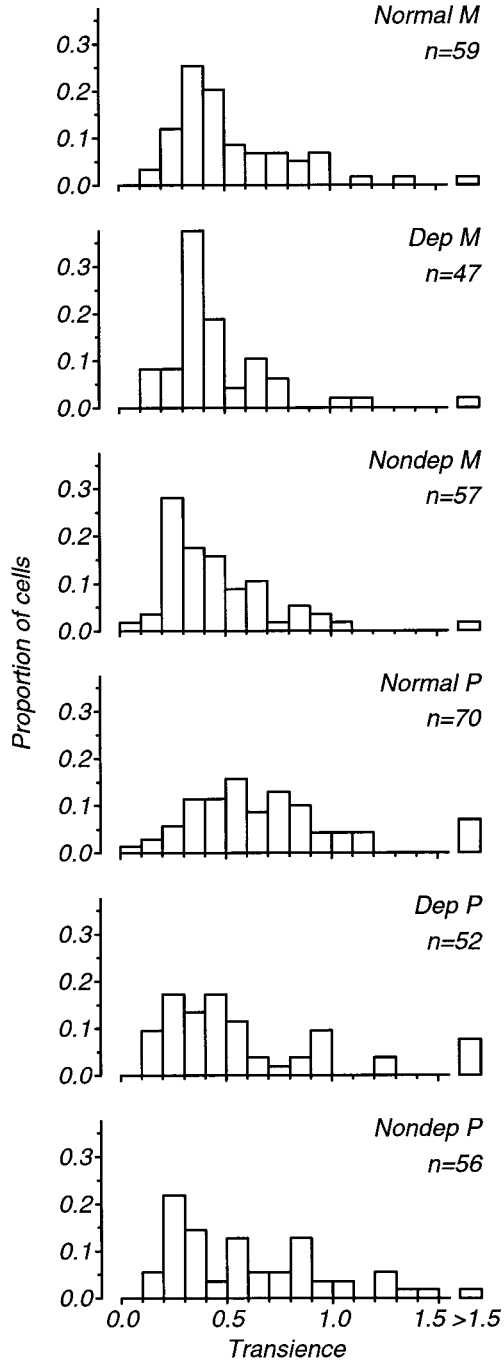


FIG. 9. Distributions of response transience indices for normal, deprived, and nondeprived magno- and parvocellular neurons. Transience is defined as the slope in log-log coordinates of the portion of the temporal frequency response function in the decade below the peak temporal frequency.

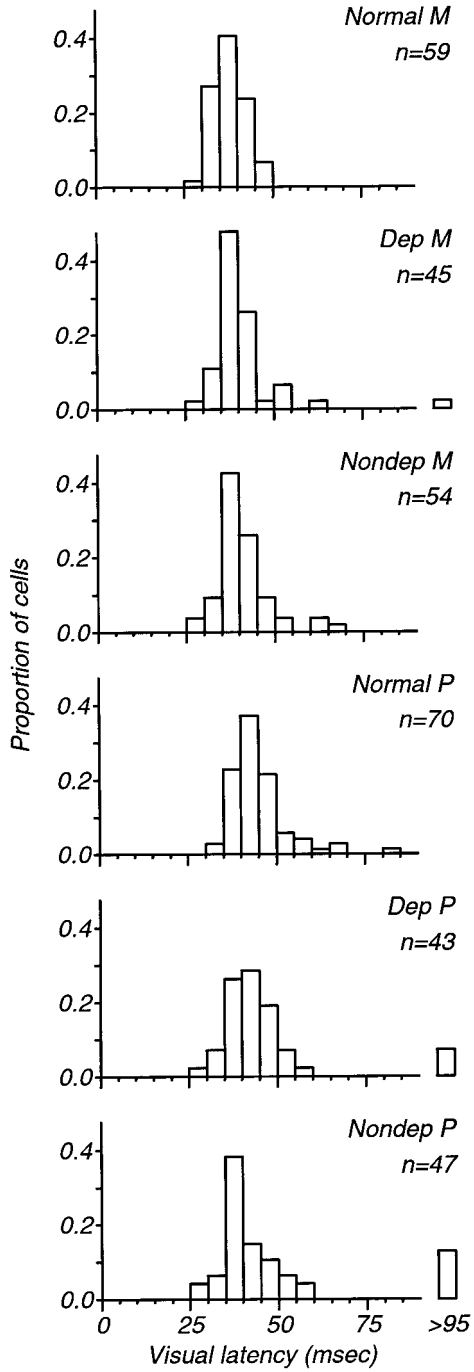


FIG. 10. Distributions of steady-state visual response latencies for normal, deprived, and nondeprived magno- and parvocellular neurons. Latency is defined as the slope of the line relating response temporal phase to stimulus temporal frequency.

and responsivity (magnocellular: deprived < nondeprived, $P < 0.033$).

DEPRIVATION EFFECTS AND STATISTICAL ANALYSES. We performed one other statistical analysis to uncover possible effects of deprivation, a logistic regression. Rather than simply using a series of two-way comparisons, this analysis allows one to take an entire *set* of measurements and shows how much predictive power each additional parameter confers when one tries to make a binary classification on the data (i.e., deprived vs. nondeprived). The set of measurements used were OX latency, center frequency ($f_c$), surround strength ($k_s$), nonlinearity, temporal frequency optimum and resolution, response latency and transience, and responsivity. This analysis, though robust, does require a full set of measurements from each cell, so any cells missing any of the set of independent measures is simply not used. One might therefore believe that the cells stable enough to obtain all measurements might represent a biased subset of our sample. We collected the full set of measurements on 60 parvo- and 79 magnocellular cells. For the magnocellular cells, a set of four measurements permitted one

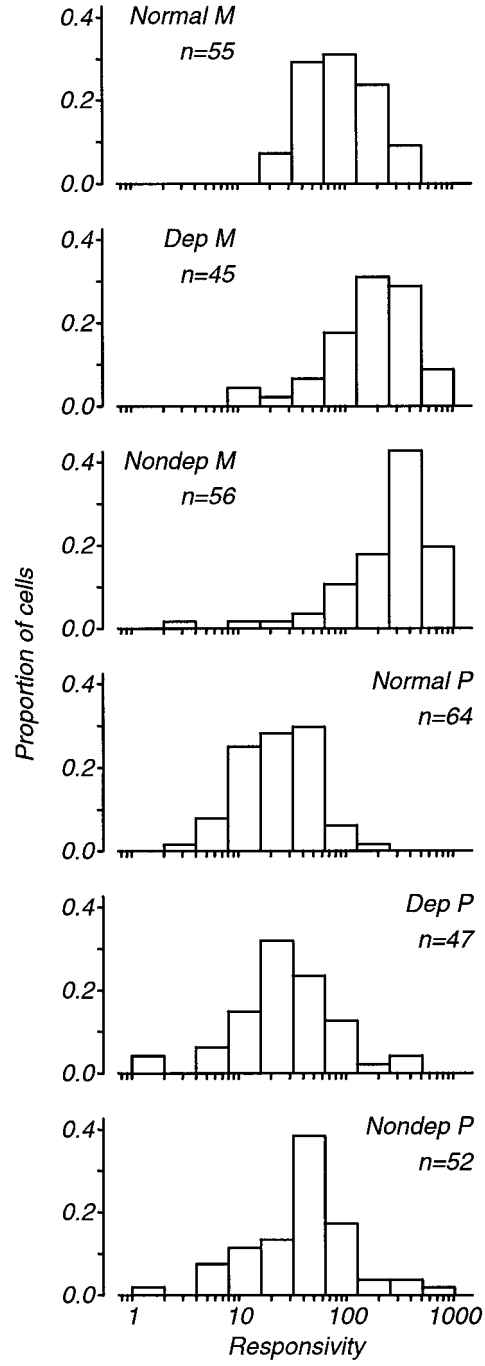


FIG. 11. Distributions of responsivity values for normal, deprived, and nondeprived magno- and parvocellular neurons. Responsivity is defined as the slope of the best-fitting contrast response function at 0 contrast.

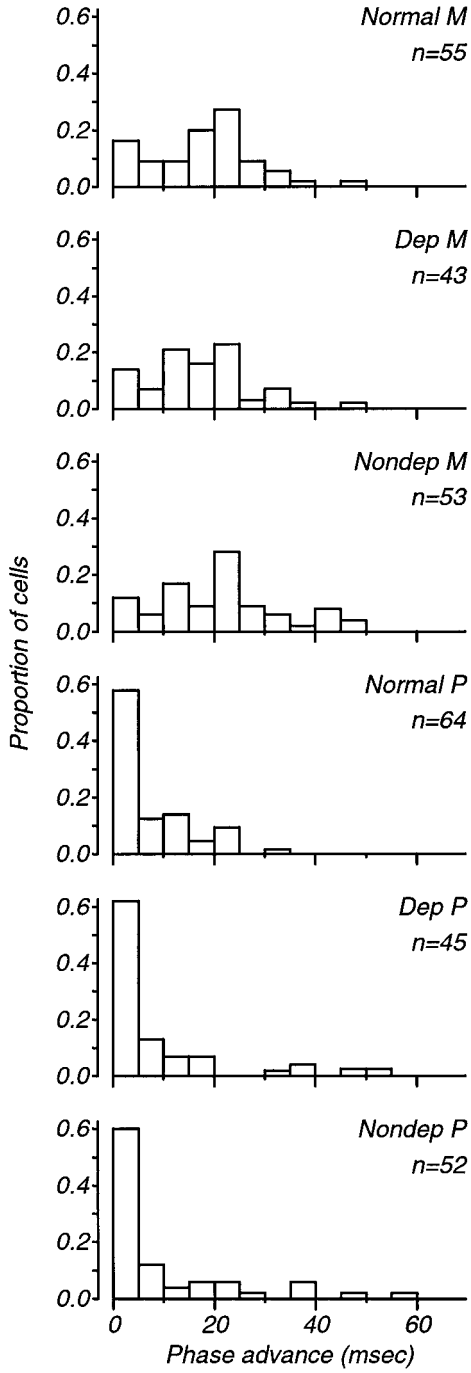


FIG. 12. Distributions of phase advance values for normal, deprived, and nondeprived magno- and parvocellular neurons. Phase advance (indicative of contrast gain control), derived from the complex function fitted to contrast response data, is the difference in response temporal phase (in ms) between the 50% contrast and blank stimulus conditions.

to predict whether a cell was deprived or nondeprived—OX latency, nonlinearity, $k_s$, and responsivity (which are the same measures shown to be affected by deprivation by simple pairwise comparisons). The coefficients and standard errors for each parameter in the final fit were OX = $-2.7 \pm 0.98$, $k_s$ = $2.7 \pm 1.32$, responsivity = $-0.002 \pm 0.0009$, nonlinearity = $-2.9 \pm 1.22$. Addition of each successive measure led to a statistically significant improvement in the $\chi^2$ test of the regression fit (using a maximum likelihood test), and addition of no other parameter improved the fit. The final model's log likelihood was $-42.3$, $\chi^2 = 84.6$, df = 74, $P = 0.187$ (i.e., the fit is not rejected and the model using 4 parameters *does* fit the data). For the parvocellular cells, no set of measurements could be used to predict the deprived/nondeprived classification, and no measure improved the $\chi^2$. Final log likelihood was $-41.4$, $\chi^2 = 82.9$, df = 59, $P = 0.022$ (i.e., the fit is rejected). Thus although pairwise comparisons for each parameter showed a few (subtle) differences between deprived and nondeprived groups, this analysis using all of the available information shows that there were no reliable effects of deprivation in the parvocellular laminae and only a few small ones in the magnocellular laminae. Our inability to uncover any major effects of monocular deprivation on the LGN can therefore not be attributed to the particular battery of statistical tests used.

## DISCUSSION

Our results confirm that parvo- and magnocellular neurons form two distinct and separate functional cell classes; we find no evidence using achromatic stimuli that these classes can usefully be subdivided. However, we also note (in agreement with Spear et al. 1994) that there is extensive overlap between magno- and parvocellular populations in most properties studied. Monocular deprivation had only very subtle effects on the visual response properties of geniculate neurons and did not seem to have specific effects on any particular cell group that we could identify.

### *Magno-parvocellular differences and evidence for subpopulations*

Our results are consistent with previous studies of the LGN showing that neurons in the magnocellular division of the LGN may be distinguished from those in the parvocellular laminae by their faster afferent conduction velocities, greater luminance contrast sensitivities, and greater contrast gain control (Blakemore and Vital-Durand 1986a; Derrington and Lennie 1984; Dreher et al. 1976; Hicks et al. 1983; Kaplan and Shapley 1982; Marrocco et al. 1982; Schiller and Malpeli 1978; Shapley et al. 1981; Spear et al. 1994). We observed a tendency for neurons with the best spatial resolution to be parvocellular and the best temporal resolution to be magnocellular. However, we found extensive overlap in spatial and temporal properties of LGN neurons, in agreement with Spear et al. (1994); this overlap can also be seen in the data of Derrington and Lennie (1984). Furthermore, the distributions of all parameters studied were unimodal and distributed continuously through the population with no clear segregation into subpopulations. Our data therefore provide no compelling evidence for distinct subgroups within the parvo- and magnocellular divisions of the monkey LGN. In particular, we find no evidence to support earlier suggestions that magnocellular neurons can be classified into distinct linear (X) and nonlinear (Y) types with high and low spatial resolutions (Blakemore and Vital-Durand 1986a; Kaplan and Shapley 1982). We emphasize again that all of these conclusions were reached using *achromatic* stimuli; chromatic opponency is one of the prime distinguishing features between the magno- and parvocellular laminae (Derrington et al. 1984; Schiller and Colby 1983; Wiesel and Hubel

1966), and we did not study the chromatic properties of these cells in any detail.

Much emphasis has been placed on the functional differences between the pathways through the parvo- and magnocellular divisions of the LGN and the different visual abilities they might mediate (Livingstone and Hubel 1988; Merigan and Maunsell 1990; Merigan et al. 1991; Schiller et al. 1990). We have shown that in many respects magno- and parvocellular functional properties overlap with subtle quantitative differences being the rule. It may therefore be problematic to assign responsibility for different visual functions to different divisions of the LGN (Livingstone and Hubel 1988; Schiller et al. 1990). Our results are therefore more consistent with Merigan's (1991) conclusion that apart from the obvious exception of color vision, which is mediated by parvocellular neurons, the parvo- and magnocellular LGN pathways both participate in most visual functions, and differ mainly in the particular range of spatiotemporal frequencies that they provide to visual cortex. Our magno- and parvocellular samples almost certainly included some koniocellular neurons, but we can rule out the possibility that differences among our magno- or parvocellular samples were masked by intrusion of koniocellular data. We compared receptive field properties of neurons located within either 50 or 100 $\mu$m of a laminar boundary to those of cells located further from the boundary; cells receiving koniocellular inputs should sit closer to laminar borders. We found *no* properties to differ as a function of distance from the laminar border.

So what is the answer to the question we raised in the introduction, "How many distinct parallel pathways involve the parvo- and magnocellular laminae of the lateral geniculate nucleus?" The short answer is two. Based on an examination of the spatiochromatic opponent organization of LGN receptive fields, Wiesel and Hubel (1966) identified three classes in the parvocellular and two in the magnocellular laminae. We have shown that full examination of these neurons' conduction velocities and spatial, temporal, and contrast processing properties using achromatic stimuli reveals each of the magno- and parvocellular divisions to be composed of one population with no compelling grounds for identifying any distinctive class. We therefore share the conclusion of Derrington and Lennie (1984) that magno- and parvocellular neurons can be divided only by chromatic properties (i.e., spatial opponency and cone inputs).

### *Anatomical effects of monocular deprivation*

As noted by many previous studies (e.g., Headon and Powell 1973; Sherman and Spear 1982; Tigges et al. 1984; Vital-Durand et al. 1978; von Noorden and Crawford 1978), cells in laminae driven by the deprived eye were pale and shrunken compared with the nondeprived-eye laminae. We also observed a decrease in immunoreactivity for the Cat-301 antigen. This decrease was most prominent in the magnocellular laminae, which seemed uniformly less reactive; we saw no sign that any subset of Cat-301-positive cells remained unaffected. This is unlike the cat, in which Cat-301 seems to specifically label Y cells, which are lost after deprivation (Guimaraes et al. 1990; Hockfield and Sur 1990; Sur et al. 1988). This may be interpreted as further evidence against the macaque magnocellular laminae containing several distinct cell classes, as all cells seemed equally affected by deprivation. Initial electron microscopic studies of the monocularly deprived macaque LGN showed no changes in the pattern of synaptic inputs to deprived versus nondeprived neurons (Wilson and Hendrickson 1981). More recently, Wilson and Forestner (1995) reexamined this issue in the squirrel monkey. They found that dendritic trees of deprived neurons were indistinguishable from those of nondeprived neurons and that deprived neurons had an essentially normal distribution of retinal and nonretinal synaptic inputs; they also observed, however, that deprived neurons had somewhat elevated synaptic densities at all distances from the soma, and most of that increase was from GABAergic synapses. This is consistent with the report by Lachica et al. (1990) that individual retinogeniculate axons in monocularly deprived galagos innervate the LGN in both deprived and nondeprived eye laminae with fewer overall boutons but at a higher density (although the change was greatest in the deprived laminae). Finally, we also note that not all chemical markers show reduced LGN activity after monocular deprivation. For example, the staining patterns for the calcium-binding proteins parvalbumin and calbindin remain unchanged (Mize et al. 1992; Tigges and Tigges 1993). The overall picture that emerges from all these studies is of subtle and selective anatomical effects in the LGN, which may plausibly be retrograde changes that arise as secondary consequences of the major reshaping of geniculate cells' axonal arbors that occurs in primary visual cortex following deprivation (LeVay et al. 1980).

### *Physiological effects of monocular deprivation*

We found only a few significant differences between the deprived and nondeprived laminae. Magnocellular neurons driven by the deprived eye had slightly faster response latencies to optic chiasm stimulation, slightly stronger receptive field surrounds, and somewhat lower responsivities. In addition, neurons in both magno- and parvocellular laminae driven by the deprived eye had lower nonlinearity indices. The drop in nonlinearity indices, while reminiscent of the Y-cell loss in cats (Sherman et al. 1972), was observed in parvocellular laminae as well, where there are no Y cells (Blakemore and Vital-Durand 1986a; Dreher et al. 1976; Kaplan and Shapley 1982; Shapley et al. 1981). Furthermore we still found nonlinear units in the deprived magnocellular laminae, again arguing against a selective subpopulation loss. It may be that the decrease in nonlinearity index, the stronger receptive field surround, and the reduction in responsivity are subtle reflections of the increase in GABAergic input to deprived neurons that has been described anatomically (Wilson and Forestner 1995).

Thus in contrast to the situation reported in the cat, the few (generally subtle) functional changes that did occur as a result of deprivation were not restricted to any one cell class. The lack of a major physiological effect of monocular deprivation on the macaque LGN is consistent with studies in other primate species also showing no effect (galagos: Sesma et al. 1984; patas monkeys: Blakemore and Vital-Durand 1986b; squirrel monkeys: Wilson and Forestner 1995). The explanation for the differing results of deprivation presumably lies in the differences in these species' visual pathways. In cats, X and Y cells are intermingled in the A laminae of the LGN, but the magnocellular C lamina is a nearly pure Y cell zone (reviewed in

Sherman 1985); it is interesting in this regard that Y axons from the deprived eye of lid sutured kittens seem to innervate the A laminae abnormally sparsely, while they innervate the C lamina normally (Sur et al. 1982), as if the effects of deprivation seen in cats are related to the opportunity of retinal X and Y axons to compete for targets during development. In primates, however, different cell classes are segregated into different laminae, so the effects of deprivation on competition between cell classes are eliminated.

A few reservations apply to our conclusions. We were not always able to isolate units easily in deprived laminae, presumably because neurons were reduced in size. Also, we occasionally encountered poorly responsive units (though we did not notice these more often in deprived vs. nondeprived laminae). It is therefore possible that we missed or undersampled a population of shrunken or abnormal cells affected by monocular deprivation. However, we explicitly tested whether encounter rates (distances in $\mu$m between successively isolated units) were different in deprived versus nondeprived laminae. None of these were significantly different from one another at the 0.01 level [nondeprived magnocellular ($160 \pm 170$, $n = 55$), deprived magnocellular ($170 \pm 190$, $n = 60$), nondeprived parvocellular ($190 \pm 200$, $n = 55$), deprived parvocellular ($120 \pm 140$, $n = 65$)]. This suggests no consistent sampling biases in deprived versus nondeprived laminae. With this caveat, we conclude that monocular deprivation has little or no effect on the functional properties of macaque LGN neurons.

### *Functional differences between macaque species*

Although in almost all respects the measured receptive field parameters in the normal animals did not differ significantly from those measured in the monocularly deprived animals, we did discover a few interesting differences. These we attribute to species differences between *M. fascicularis* and *M. mulatta*. *1*) On-off cells: the proportions of on- and off-center cells and their distribution across LGN laminae differed (see Table 2). Although both species' *P* laminae consisted mainly of on cells, laminae 5 and 6 in *M. mulatta* consisted almost entirely of on cells [in agreement with Schiller and Malpeli (1978); though we do find laminae 3 and 4 more nearly balanced between on and off cells]. In *M. fascicularis*, however, it seemed that this prominence of on cells in laminae 5 and 6 was less pronounced. *2*) Response transience: we found cells to be slightly more transient in *M. fascicularis* than in *M. mulatta* for both magno- and parvocellular groups (Fig. 9). *3*) Responsivity: LGN cells (in both M and P divisions) of *M. fascicularis* were on average consistently less responsive than were those in either deprived or nondeprived laminae of *M. mulatta* (see Fig. 11). *4*) Variation of spatial properties with eccentricity: although $f_c$ values decreased and $r_c$ values increased with eccentricity in both the normal and monocularly deprived animals, this trend was less obvious in the deprived animals. This was due primarily to the presence in the deprived animals' parvocellular laminae of neurons at low eccentricities with large receptive field centers (although the smallest receptive field centers were in the same range as the normal animals). We are unsure whether the presence of these neurons can be attributed to the deprivation regimen. However, both Spear et al. (1994), who studied normal *M. mulatta*, and Derrington and Lennie (1984), who studied normal *M. fascicularis*, also showed that within the central 10° there was only a weak dependence on eccentricity of spatial resolution or receptive field center radius; as in this study, this reflected the presence of neurons in the parvocellular laminae with both large and small receptive field centers. As the methods used to measure these parameters and to determine receptive field eccentricity were exactly the same in both sets of animals, we assume that the species differences noted here are genuine. We emphasize that these effects cannot be attributed to the deprivation regimen as the values reported here are within the range of normal values for *M. mulatta* reported by others (see, for example, Spear et al. 1994). We are uncertain of the functional significance of any of these species differences.

### *Implications for homology*

Parallel processing streams from retina through the LGN to visual cortex are a prominent feature of the visual pathways of primates and carnivores, and an enduring issue is the evolutionary relationship between the W, X, and Y pathways of carnivores and the konio-, parvo-, and magnocellular pathways of primates. Two different homologies have been advanced. In one, Shapley and Perry (1986) have suggested that W cells are the homologue of parvocellular cells, and that X and Y cells together are homologous to magnocellular cells, with no specific suggestion for the koniocellular path. This was based largely on evidence that the magnocellular laminae contained two distinct classes with excellent contrast sensitivity but differing in linearity of spatial summation (e.g., like X and Y cells) and that the parvocellular laminae contained cells with poor contrast sensitivity (e.g., "sluggish" in responsiveness, like W cells). We did not find distinct X- and Y-like classes in the magnocellular laminae, and our data therefore do not support this view.

In the other hypothesis (Casagrande 1994; Dreher et al. 1976; Sherman et al. 1976), the suggested homologies are W to konio, X to parvo, and Y to magno. This is based largely on several morphological features: the relative sizes of the cells and axons is similar, increasing from W to X to Y and from konio to parvo to magno; projection patterns to striate cortex, since Y and magnocellular axons tend to terminate more dorsally within layer 4 than do X and parvocellular axons, respectively, and both W and koniocellular axons innervate cytochrome oxidase-rich "blobs" in layer 3; and CAT-301 labeling is found fairly selectively in Y and magnocellular cells. Our data are more consistent with this second view of homology.

We are grateful to M. Carandini, S. Fenstemaker, and J. Sullivan for assistance and to S. Hockfield for supplying the Cat-301 antibody.

This work was supported by National Eye Institute Grants EY-01916, EY-02017, EY-02545, EY-03038, and EY-11409.

Present addresses: J. B. Levitt, Dept. of Biology, City College of New York, 138th St. and Convent Ave., New York, NY 10031; R. A. Schumer, Dept. of Ophthalmology, Mount Sinai School of Medicine, One Gustave Levy Place, New York, NY 10029; P. D. Spear, Dept. of Psychology, University of Colorado, Boulder, CO 80309-0275.

## REFERENCES

BLAKEMORE C AND VITAL-DURAND F. Organization and post-natal development of the monkey's lateral geniculate nucleus. *J Physiol (Lond)* 380: 453–491, 1986a.

BLAKEMORE C AND VITAL-DURAND F. Effects of visual deprivation on the development of the monkey's lateral geniculate nucleus. *J Physiol (Lond)* 380: 493–511, 1986b.

CARANDINI M, HEEGER DJ, AND MOVSHON JA. Linearity and normalization in simple cells of the macaque primary visual cortex. *J Neurosci* 17: 8621–8644, 1997.

CASAGRANDE VA. A third parallel visual pathway to primate area V1. *Trends Neurosci* 17: 305–310, 1994.

CLARK WEL. The laminar organization and cell content of the lateral geniculate body in the monkey. *J Anat* 75: 419–433, 1941.

DERRINGTON AM, KRAUSKOPF J, AND LENNIE P. Chromatic mechanisms in lateral geniculate nucleus of macaque. *J Physiol (Lond)* 357: 241–265, 1984.

DERRINGTON AM AND LENNIE P. Spatial and temporal contrast sensitivity of neurones in lateral geniculate nucleus of macaque. *J Physiol (Lond)* 357: 219–240, 1984.

DREHER B, FUKADA Y, AND RODIECK RW. Identification, classification and anatomical segregation of cells with X-like and Y-like properties in the lateral geniculate nucleus of old-world primates. *J Physiol (Lond)* 258: 433–452, 1976.

ENROTH-CUGELL C AND ROBSON JG. The contrast sensitivity of retinal ganglion cells of the cat. *J Physiol (Lond)* 187: 517–552, 1966.

FITZPATRICK DC, ITOH K, AND DIAMOND IT. The laminar organization of the lateral geniculate body and the striate cortex in the squirrel monkey (Saimiri sciureus). *J Neurosci* 3: 673–702, 1983.

GUIMARAES A, ZAREMBA S, AND HOCKFIELD S. Molecular and morphological changes in the cat lateral geniculate nucleus and visual cortex induced by visual deprivation are revealed by monoclonal antibodies Cat-304 and Cat-301. *J Neurosci* 10: 3014–3024, 1990.

HEADON MP AND POWELL TPS. Cellular changes in the lateral geniculate nucleus of infant monkeys after suture of the eyelids. *J Anat* 116: 135–145, 1973.

HENDRY SHC, HOCKFIELD S, JONES EG, AND MCKAY R. Monoclonal antibody that identifies subsets of neurones in the central visual system of monkey and cat. *Nature* 307: 267–269, 1984.

HENDRY SHC, JONES EG, HOCKFIELD S, AND MCKAY RDG. Neuronal populations stained with the monoclonal antibody cat-301 in the mammalian cerebral cortex and thalamus. *J Neurosci* 8: 518–542, 1988.

HENDRY SHC AND YOSHIOKA T. A neurochemically distinct third channel in the macaque dorsal lateral geniculate nucleus. *Science* 264: 575–577, 1994.

HICKS TP, LEE BB, AND VIDYSAGAR TR. The responses of cells in macaque lateral geniculate nucleus to sinusoidal gratings. *J Physiol (Lond)* 337: 183–200, 1983.

HOCHSTEIN S AND SHAPLEY RM. Quantitative analysis of retinal ganglion cell classifications. *J Physiol (Lond)* 262: 237–264, 1976.

HOCKFIELD S, MCKAY RD, HENDRY SHC, AND JONES EG. A surface antigen that identifies ocular dominance columns in the visual cortex and laminar features of the lateral geniculate nucleus. *Cold Spring Harb Symp Quant Biol* 48: 877–889, 1983.

HOCKFIELD S AND SUR M. Monoclonal antibody Cat-301 identifies Y-cells in the dorsal lateral geniculate nucleus of the cat. *J Comp Neurol* 300: 320–330, 1990.

KAPLAN E AND SHAPLEY RM. X and Y cells in the lateral geniculate nucleus of macaque monkeys. *J Physiol (Lond)* 330: 125–143, 1982.

LACHICA EA, CROOKS MW, AND CASAGRANDE VA. Effects of monocular deprivation on the morphology of retinogeniculate axon arbors in a primate. *J Comp Neurol* 296: 303–323, 1990.

LEE BB, POKORNY J, SMITH VC, AND KREMERS J. Responses to pulses and sinusoids in macaque ganglion cells. *Vision Res* 34: 3081–3096, 1994.

LEHMKUHLE S, KRATZ KE, MANGEL SC, AND SHERMAN SM. Effects of early monocular lid suture on spatial and temporal sensitivity of neurons in dorsal lateral geniculate nucleus of the cat. *J Neurophysiol* 43: 542–556, 1980.

LENNIE P. Parallel visual pathways. *Vision Res* 20: 561–594, 1980.

LEVAY S, WIESEL TN, AND HUBEL DC. The development of ocular dominance columns in normal and visually deprived monkeys. *J Comp Neurol* 191: 1–51, 1980.

LEVITT JB, MOVSHON JA, SHERMAN SM, AND SPEAR PD. Effects of monocular deprivation on macaque LGN. *Invest Ophthalmol Vis Sci Suppl* 30: 296, 1989.

LIVINGSTONE M AND HUBEL D. Segregation of form, color, movement, and depth—anatomy, physiology, and perception. *Science* 240: 740–749, 1988.

MARROCCO RT, MCCLURKIN JW, AND YOUNG RA. Spatial summation and conduction latency classification of cells of the lateral geniculate nucleus of macaques. *J Neurosci* 2: 1275–1291, 1982.

MERIGAN WH. P and M pathway specialization in the macaque. In: *From Pigments to Perception*, edited by Valberg A and Lee BB. New York: Plenum, 1991, p. 117–125.

MERIGAN WH, KATZ LM, AND MAUNSELL JHR. The effects of parvocellular lateral geniculate lesions on the acuity and contrast sensitivity of macaque monkeys. *J Neurosci* 11: 994–1001, 1991.

MERIGAN WH AND MAUNSELL JHR. Macaque vision after magnocellular lateral geniculate lesions. *Vis Neurosci* 5: 347–352, 1990.

MERRILL EG AND AINSWORTH A. Glass-coated platinum-plated tungsten microelectrode. *Med Biol Eng* 10: 495–504, 1972.

MIZE RR, LUO Q, AND TIGGES M. Monocular enucleation reduces immunoreactivity to the calcium binding protein calbindin 28kD in the *Rhesus* monkey lateral geniculate nucleus. *Vis Neurosci* 9: 471–482, 1992.

RODIECK RW. Quantitative analysis of cat retinal ganglion cell response to visual stimuli. *Vision Res* 5: 583–601, 1965.

RODIECK RW AND BRENING RK. Retinal ganglion cells—properties, types, genera, pathways and trans-species comparisons. *Brain Behav Evol* 23: 121–164, 1983.

SCHILLER PH AND COLBY CL. The responses of single cells in the lateral geniculate nucleus of the rhesus monkey to color and luminance contrast. *Vision Res* 23: 1631–1641, 1983.

SCHILLER PH, LOGOTHETIS NK, AND CHARLES ER. Functions of the color-opponent and broad-band channels of the visual system. *Nature* 343: 68–70, 1990.

SCHILLER PH AND MALPELI JG. Functional specificity of lateral geniculate nucleus laminae of the rhesus monkey. *J Neurophysiol* 41: 788–797, 1978.

SESMA MA, IRVIN GE, KUYK TK, NORTON TT, AND CASAGRANDE VA. Effects of monocular deprivation on the lateral geniculate nucleus in a primate. *Proc Natl Acad Sci USA* 81: 2255–2259, 1984.

SESTOKAS AK AND LEHMKUHLE S. Visual response latency of X- and Y-cells in the dorsal lateral geniculate nucleus of the cat. *Vision Res* 26: 1041–1054, 1986.

SHAPLEY R AND HOCHSTEIN S. Visual spatial summation in two classes of geniculate cells. *Nature* 256: 411–413, 1975.

SHAPLEY RM, KAPLAN E AND SOODAK R. Spatial summation and contrast sensitivity of X- and Y-cells in the lateral geniculate nucleus of the macaque. *Nature* 292: 543–545, 1981.

SHAPLEY RM AND PERRY VH. Cat and monkey retinal ganglion cells and their visual functional roles. *Trends Neurosci* 9: 229–235, 1986.

SHAPLEY RM AND VICTOR JD. The effect of contrast on the transfer properties of cat retinal ganglion cells. *J Physiol (Lond)* 285: 275–298, 1978.

SHERMAN SM. Functional organization of the W-cell, X-cell, and Y-cell pathways in the cat—a review and hypothesis. *Prog Psychobiol Physiol Psych* 11: 233–314, 1985.

SHERMAN SM, HOFFMAN K-P, AND STONE J. Loss of a specific cell type from dorsal lateral geniculate nucleus in visually deprived cats. *J Neurophysiol* 35: 532–541, 1972.

SHERMAN SM, SCHUMER RA, AND MOVSHON JA. Functional cell classes in the macaque's LGN. *Soc Neurosci Abstr* 10: 296, 1984.

SHERMAN SM AND SPEAR PD. Organization of visual pathways in normal and visually deprived cats. *Physiol Rev* 62: 738–855, 1982.

SHERMAN SM, WILSON JR, KAAS JH, AND WEBB SV. X- and Y-cells in the dorsal lateral geniculate nucleus of the owl monkey (*Aotus trivirgatus*). *Science* 192: 475–477, 1976.

SO YT AND SHAPLEY R. Is there an effect of monocular deprivation on the proportions of X and Y cells in the cat lateral geniculate nucleus? *Exp Brain Res* 39: 41–49, 1980.

SPEAR PD, MOORE RJ, KIM CBY, XUE JT, AND TUMOSA N. Effects of aging on the primate visual system: spatial and temporal processing by lateral geniculate neurons in young adult and old rhesus monkeys. *J Neurophysiol* 72: 402–420, 1994.

STONE J. *Parallel Processing in the Visual System: The Classification of Retinal Ganglion Cells and Its Impact on the Neurobiology of Vision*. New York: Plenum, 1983.

STONE J, DREHER B, AND LEVENTHAL A. Hierarchical and parallel mechanisms in the organization of visual cortex. *Brain Res Rev* 1: 345–394, 1979.

SUR M, FROST D, AND HOCKFIELD S. Expression of a surface-associated antigen on Y-cells in the cat lateral geniculate nucleus is regulated by visual experience. *J Neurosci* 8: 874–882, 1988.

SUR M, HUMPHREY AL, AND SHERMAN SM. Monocular deprivation affects X- and Y-cell retinogeniculate terminations in cats. *Nature* 300: 183–185, 1982.

TIGGES M, HENDRICKSON AE, AND TIGGES J. Anatomical consequences of long-term monocular eyelid closure on lateral geniculate nucleus and striate cortex in squirrel monkey. *J Comp Neurol* 227: 1–13, 1984.

TIGGES M AND TIGGES J. Parvalbumin immunoreactivity in the lateral genic-

ulate nucleus of rhesus monkeys raised under monocular and binocular deprivation conditions. *Vis Neurosci* 10: 1043–1053, 1993.

VITAL-DURAND F, GAREY LJ, AND BLAKEMORE C. Monocular and binocular deprivation in the monkey: morphological effects and reversibility. *Brain Res* 158: 45–64, 1978.

VON NOORDEN GK AND CRAWFORD MLJ. Morphological and physiological changes in the monkey visual system after short-term lid suture. *Invest Ophthalmol Vis Sci* 17: 762–768, 1978.

WALLS GL. *The Vertebrate Eye and Its Adaptive Radiation.* Bloomfield Hills, MI: Cranbrook, 1942.

WIESEL TN AND HUBEL DH. Spatial and chromatic interactions in the lateral geniculate body of the rhesus monkey. *J Neurophysiol* 29: 1115–1156, 1966.

WIESEL TN AND RAVIOLA E. Myopia and eye enlargement after neonatal lid fusion in monkeys. *Nature* 266: 66–68, 1977.

WILSON JR AND FORESTNER DM. Synaptic inputs to single neurons in the lateral geniculate nuclei of normal and monocularly deprived squirrel monkeys. *J Comp Neurol* 362: 468–488, 1995.

WILSON JR AND HENDRICKSON AE. Neuronal and synaptic structure of the dorsal lateral geniculate nucleus in normal and monocularly deprived Macaca monkeys. *J Comp Neurol* 197: 517–539, 1981.